Investigation of the prefrontal cortical structure and function following ablation of autophagy in projection neurons during adolescence

Lito Parapera Papantoniou (421)

MSc Program: Molecular Biology – Biomedicine
University of Crete, School of Biology
Institute of Molecular Biology & Biotechnology (IMBB) of the Foundation for Research and Technology Hellas (FORTH)

Supervisors:

Associate Professor Kyriaki Sidiropoulou
Dr. Vassiliki Nikoletopoulou
Associate Professor Ioannis Charalampopoulos

Heraklion, 2021

Abstract

Autophagy is a cellular process that promotes the removal of dysfunctional or unnecessary products via lysosome-dependent pathways. Autophagy has been associated with the mechanisms underlying the pruning of excitatory synapses that normally occurs during development and it is believed that its dysregulation could lead to neurodevelopmental diseases. The prefrontal cortex is a brain area involved in higher-order cognitive function and exhibits slower maturation compared to other cortical areas. Here, we aimed to understand whether inhibiting autophagy during the synaptic pruning period of the PFC (post-natal day (P)35-p45) affects dendritic spine density in the PFC and its function. For this purpose, *thy1-Cre^{ERT2};atg5$^{f/f}$* (KO) mice were generated, which lack *Atg5*-a gene necessary for the elongation of the phagophore during the process of autophagy-in projection neurons expressing Thy1. Tamoxifen (tmx) was post-injected to mice on P31-35 or P61-65 (as a control), to induce Cre activity and lead to autophagy impairment. A milder autophagy impairment was enabled in *thy1-Cre^{ERT2};atg5$^{+/fl}$ (*heterozygotes or Het*)* animals. After P80, all mice were tested in the following: Novel Object Recognition (NOR), Object-To-Place (OTP), Temporal Order Object Recognition (TOR) tasks, and Three-Chamber Sociability test. Dendritic spine morphology and density of these animals' pyramidal neurons were studied using optical microscopy following Golgi-cox staining. A tendency towards increased spine densities, especially in the case of mature spines, in the PFC of animals whose neuronal autophagy was impaired during adolescence (P31-P35) or early adulthood (P61-P65) was observed. Autophagy impairment during adolescence or early adulthood did not exert significant effects on sociability or social memory. However, neuronal autophagy impairment during adolescence resulted in recency and spatial memory deficits, as well as in deficits in novelty-recognition. Deficits in spatial memory were also observed in animals with impaired autophagy during early adulthood. Therefore, our results suggest that deficient autophagy after P30 results in increased dendritic spine density in the PFC and impaired performance in NOR, OTP, and TOR tasks.

Περίληψη

Η αυτοφαγία συνιστά μία κυτταρική διαδικασία η οποία συνεισφέρει στην απομάκρυνση δυσλειτουργικών ή μη χρήσιμων προϊόντων μέσω του λυσοσσωμικού μονοπατιού. Η αυτοφαγία έχει συσχετιστεί με τους μηχανισμούς που διέπουν το κλάδεμα (pruning) των διεγερτικών συνάψεων στον εγκέφαλο, το οποίο συμβαίνει φυσιολογικά κατά την ανάπτυξη, ενώ θεωρείται πως διαταραχές στο pruning μπορούν να οδηγήσουν στην εκδήλωση νευροαναπτυξιακών ασθενειών. Ο προμετωπιαίος φλοιός είναι μια εγκεφαλική περιοχή που υποστηρίζει ανώτατες γνωστικές, εκτελεστικές λειτουργίες και εμφανίζει μία πιο χρονικά παρατεταμένη ανάπτυξη συγκριτικά με άλλες φλοιϊκές περιοχές. Στη συγκεκριμένη μελέτη προσπαθήσαμε να μελετήσουμε κατά πόσον η παρεμπόδιση της αυτοφαγίας κατά την περίοδο του συναπτικού pruning στον προμετωπιαίο φλοιό-μεταγεννητικές μέρες (postatal days or P) 31-42 (P31-P24)-επηρεάζει την πυκνότητα των δενδριτικών ακανθών στον προμετωπιαίο φλοιό, καθώς και τη λειτουργία του. Για το σκοπό αυτό, δημιουργήθηκαν οι *thy1-Cre^{ERT2};atg5$^{f/f}$* διαγονιδιακοί μύες, από τους οποία λείπει το *Atg5* γονίδιο, υπεύθυνο για την επιμήκυνση του φαγοφόρου κατά τη διαδικασία της αυτοφαγίας, από τους προβλητικούς τους νευρώνες. Πραγματοποιήθηκαν ενέσεις ταμοξιφαίνης κατά τις P31-P35 και P61-P65 (πρώιμη ενήλικη ζωή, control) ημέρες, προκειμένου να ενεργοποιηθεί η δραστηριότητα της Cre ρεκομπινάσης και να παρεμποδιστεί η αυτοφαγία. Οι ετερόζυγοι *thy1-Cre^{ERT2};atg5$^{+/f}$* μύες εμφάνισαν πιο ήπια μείωση της αυτοφαγίας. Μετά το P80, όλοι οι μύες ελέγχθηκαν στις εξής δοκιμασίες: δοκιμασία αναγνώρισης νέου αντικειμένου, δοκιμασία αναγνώρισης θέσης του αντικειμένου, και δοκιμασία αναγνώρισης αντικειμένου σε χρονική σειρά. Η μορφολογία και η πυκνότητα των δενδριτικών ακανθών των πυραμιδικών νευρώνων των συγκεκριμένων μυών μελετήθηκε με οπτική μικροσκοπία έπειτα από χρώση Golgi-cox. Παρατηρήθηκε μία τάση προς αυξημένες πυκνότητες δενδριτικών ακανθών, ιδιαίτερα των ώριμων ακανθών, στον προμετωπιαίο φλοιό μυών των οποίων η αυτοφαγία είχε παρεμποδιστεί κατά την εφηβεία (P31-P35) ή κατά την πρώιμη ενήλικη ζωή (P61-P65). Η κοινωνικότητα και η κοινωνική μνήμη των μυών δεν επηρεάστηκε σημαντικά από τη μειωμένη αυτοφαγία ούτε κατά την εφηβεία, ούτε κατά την πρώιμη ενηλικίωση. Ωστόσο, η μείωση της αυτοφαγίας κατά την εφηβεία οδήγησε σε ελλείμματα της χρονικής και της χωρικής μνήμης, καθώς και της ικανότητας αναγνώρισης νέων αντικειμένων. Ελλείμματα στην χωρική μνήμη παρατηρήθηκαν ακόμα και κατά τη μείωση της αυτοφαγίας στην πρώιμη ενήλικη ζωή. Επομένως, τα αποτελέσματά μας προτείνουν ότι μειωμένη αυτοφαγία μετά το P30 προκαλεί αύξηση της πυκνότητας των δενδριτικών ακανθών στον προμετωπιαίο φλοιό, καθώς επίσης και μειωμένη απόδοση στις δοκιμασία αναγνώρισης νέου αντικειμένου, αναγνώρισης θέσης του αντικειμένου, και αναγνώρισης αντικειμένου σε χρονική σειρά.

Acknowledgments

Many people contributed to the completion of the present Diploma thesis, each one in their own way. I would first like to thank my supervisor and associate Professor at the University of Crete (UoC), Kyriaki Sidiropoulou, for allowing me to conduct my Diploma thesis in the laboratory of "Neurophysiology and Behavior" at the UoC collaborating with the Institute for Molecular Biology & Biotechnology of the Foundation for Research and Technology Hellas (IMBB-FORTH). Her constant support and belief in me while still having little neuroscience background inspired me to try my best every day.

I would also like to thank Professor Ioannis Charalampopoulos and Dr. Vassiliki Nikoletopoulou for accepting to become members of my thesis committee.

Moving on to my co-workers, I would like to thank Maria Plataki and Vicky Stavroulaki for their help with behavioral experiments and Golgi-cox staining. Kostas Diskos, Dora Asimi, Aggeliki Velli, Lida Vagiaki, Olga Lyraki, and Chrysa Iordanidou also provided important support. Working with all of you was a real pleasure. Also, Niki Ktena's contribution to tamoxifen manipulations and consulting on the project was significant. At this point, I would like to thank Ifigeneia Ioannidi, a good friend of mine who I had the luck to meet at the laboratory and who became the best lab partner I could ask for. (Lab) life during a pandemic would not be that fun without you.

I could not help but also thank my childhood and university friends for always cheering me up and patiently listening to my grumbling. I promise to make it up to you with a covid-free gathering. Last but not least, I would like to express my gratitude to my family for their sacrifices and unconditional love and support. Without them, I would not be able to be where I am today.

Table of Contents

A. Theoretical background

A.1 The Nervous System

Nervous tissue is found in the majority of living organisms, ranging from single nerve nets in Hydra (Dupre and Yuste 2017) to multiple interconnected, myelinated brain circuits in mammals. From receiving and processing stimuli, to performing complex cognitive functions, the nervous system allows for efficient survival and adjustment to the constantly changing environment. On an anatomic basis, the Nervous System of vertebrates can be divided into the Central Nervous System (CNS), consisting of the brain and the spinal cord, and the Peripheral Nervous System, mainly comprising nerves that connect the CNS with every part of the body. It is well established that, the higher the position of an organism in the scale of evolution, the more complicated its nervous system (Brodal 2004).

Neurons, the electrical signal-propagating cells of the nervous system, constitute fundamental units that communicate with each other via synapses. Their nucleus is enclosed in a structure called soma, out of which an elongated structure, the axon, as well as branch-like structures, the dendrites, emerge. The axon propagates electrical signals to the neurons' terminals, which can be transmitted to adjacent neurons. The dendrites are considered responsible for integrating electrical inputs via small protrusions on their membrane, the so-called dendritic spines (Kandel 2013). Additional information on the morphology and the role of dendritic spines is given in the 'Synaptic pruning' sub-section. In case the electrical signal a neuron receives surpasses a certain threshold, an action potential is generated near the soma of the neuron and it travels along the axon, to result in the secretion of a neurotransmitter in the synaptic cleft that acts on the membrane of a target neuron. In the mature brain, glutamate and γ-aminobutyric acid (GABA) are the main excitatory and inhibitory neurotransmitters respectively (Kandel 2013).

Glial cells, non-electrically excitable cells, communicate with neurons and exert important functions. Their role was initially limited to the production of myelin-a lipid-rich substance that insulates the axon and increases the rate of signal transduction-and to providing neurons with nutrients and support. However, an increasing number of studies now link their role with synaptogenesis and synaptic plasticity (He and Sun 2007).

A.2 The Central Nervous System (CNS) Development

During prenatal and postnatal life, the immature brain undergoes fundamental procedures that align with the broader concept of development. The main phenomena that fall into this category include, in temporal order, the processes of neurogenesis, neuronal migration, gliogenesis, synaptogenesis, myelination, and synaptic pruning. These overlapping, key neurodevelopmental events are depicted in **Figure 1**. In humans, prenatal development can be divided into the embryonic, comprising the first 8 weeks of pregnancy, and fetal, comprising the last month of pregnancy, stages. During the embryonic period, the CNS primordium arises. The notochord formation is followed by the induction of the neural plate within the ectoderm. Neural folds that arise along the neural plate's midline on the 23rd postconceptional day (pcd) lead to the formation of the neural groove. Later on, the neural tube is formed initially in the center of the neural plate and then proceeds rosto-caudally. Along this axis, the neural tube grows unequally, and therefore, it is patterned into the following anatomically distinct areas:

forebrain, midbrain, and hindbrain. The spinal cord is formed in the caudal area and the neural tube gets also patterned along the dorsal-ventral axis to result in the establishment of neuron progenitors that give rise to specific neural cell types. On the other hand, the fetal stage of development marks the onset of organogenesis (Silbereis et al. 2016).

The term neurogenesis refers to the generation of neurons by neural stem cells (NSCs). During human embryonic development, NSCs residing in the neural tube start to proliferate, and, upon a density population, these now-called neuroepithelial cells (NECs) transform into elongated, radial glial cells (RGCs). RGCs are maintained in the embryonic ventricular zone and their further proliferation status results in the production of neurons, either directly, or indirectly through the generation of intermediate neuronal progenitors (INPs). Adult neurogenesis is also observed in certain brain regions, such as the hippocampus (Breunig, Haydar, and Rakic 2011).

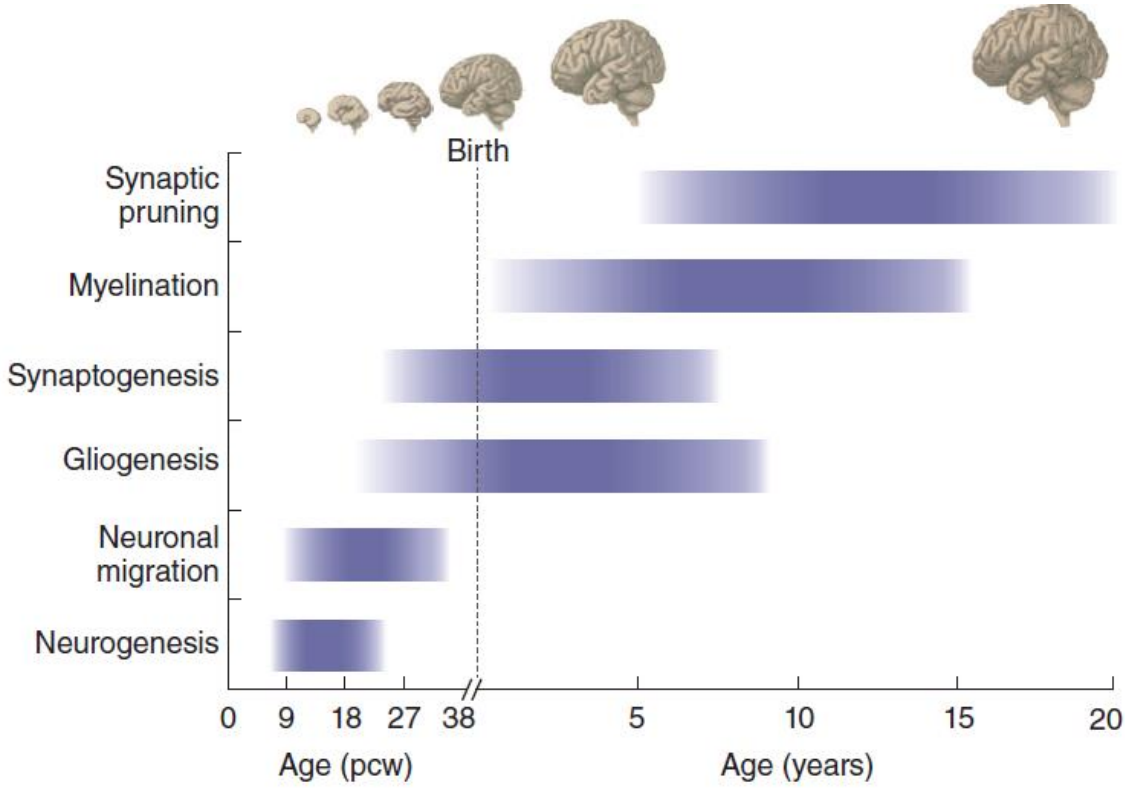

Figure 1: Graphical representation of key events in human neurodevelopment. The above graph depicts the approximate time periods when the processes of neurogenesis, neuronal migration, gliogenesis, synaptogenesis, myelination, and synaptic pruning take place in humans. The illustrations roughly show the morphology and relative size of the human brain in respect to time (Marín 2016).

Neurons, however, are not integrated into neural circuits directly after their generation, as they first have to migrate to distinct locations and mature. This migration process is regulated by chemoattractive, chemorepulsive, and mitogenic cues expressed by glial cells that reside in the neural microenvironment. Specific receptors in distinct areas of the growing axons, the so-called growth cones, bind selectively to these molecules, thus contributing to the process of neural wiring. Of note is the fact that developing axons depend on intermediate targets that express these guidance molecules (e.g. Ephrins, Netrins, Semaphorins) at the appropriate times and locations (Bellon and Mann 2018).
During human embryonic development, the process of gliogenesis follows neurogenesis and it is continued in later postnatal life. In particular, RGCs give rise to astrocyte and oligodendrocyte precursor cells in midgestation (Howard et al. 2008). Oligodendrocytes are mainly generated in the first 3

postnatal years when they mature and migrate in parallel with the process of myelination (Jakovcevski et al. 2009). Mature astrocytes are observed as early as 15 pcw in the neocortex and they are generated by the direct differentiation and subsequent proliferation of RGCs (Choi and Lapham 1978). Their differentiation process reaches its peak in the first 3 postnatal years of life, where they exert roles in the formation and elimination of synapses (Clarke and Barres 2013).

In the human CNS, myelin is generated by oligodendrocyte precursor cells (OPCs) that migrate, proliferate, and differentiate towards mature oligodendrocytes around the 3rd trimester of fetal life (Kuhn et al. 2019). However, until birth, the myelin levels are remarkably limited, and they increase progressively during infancy and until early adulthood. Myelination can also continue in certain brain areas, such as the cerebral cortex, throughout adult life (Choi 1981; Schmithorst et al. 2002; Westlye et al. 2010; Slater et al. 2019; Sexton et al. 2014). The timing and rate of myelination differ among distinct neural fibers and it depends on their subsequent functionality. Functionally relevant networks undergo synchronized changes in their myelination status throughout lifespan (Buyanova and Arsalidou 2021). Myelination exerts a prominent role in synaptic plasticity and its dynamics have been shown to shape by experience and learning (Fields 2015).

In order for neural circuits to be assembled, simple neural connections first need to be established. In mammals, synaptogenesis, that is the generation of neuronal connections, initiates early, at the transition from embryonic to fetal life (Silbereis et al. 2016). However, the majority of synapses and circuits that are formed during this period are transient, with the peak of synaptogenesis in the neocortex occuring during the prenatal and early postnatal life (Huttenlocher 1979). The very first synapses are found in the cervical spinal cord around 44 pcd, while, within the developing neocortex, synapses start to form in the preplate between the 4th and 5th pcw (Okado, Kakimi, and Kojima 1979; Zecevic 1998). Around 10 pcw, neocortical synaptogenesis is primarily performed in the subplate (SP) (Hoerder-Suabedissen and Molnár 2015), a fundamental cortical zone along with the subventricular zone (SVZ), intermediate zone (IZ), and cortical plate (CP). The elementary features of the pyramidal apical and basal dendrites start to emerge at approximately 15 pcw (Mrzljak et al. 1988), however, dendritic spines appear in neocortical pyramidal neurons and interneurons between the 24th and 27th pcw, after the establishment of thalamocortical interactions in the CP (Kostovic and Rakic 1990). In parallel with this outgrowth of thalamocortical afferents, dendrites ramify intensively, and they form synapses with the pyramidal neurons of future layers III and V (more information on neocortical layers is given later on ‘The Prefrontal Cortex’ sub-section) (Mrzljak et al. 1988). During this period, the typical six-layers organization of the neocortex starts to occur in the CP. In all mammals, the pyramidal neurons in the CP should encode spatial information concerning their laminar position and their cortical area identity. Several mouse studies indicate that the latter is feasible via a graded expression pattern of transcription factors that is followed by excessive thalamic input (Shibata, Gulden, and Sestan 2015; Chou et al. 2013).

Increased rates of synaptogenesis are maintained during the first postnatal years, where elimination of excitatory synapses, the so-called synaptic pruning, also emerges to result in reorganization of the neural circuitry. Different brain regions mature at different times and therefore, synaptic pruning can continue even during the third decade of life, in areas like the prefrontal cortex (Petanjek et al. 2011).

A.3 Synaptic pruning

A.3.1 Definition and influencing factors

Synaptic pruning promotes the removal of unnecessary or damaged connections in the developing brain. Adolescence marks an important period for the transition to adult life, which is characterized by augmented cognitive ability and complex emotional function. Indeed, the massive wave of synapse elimination that follows the initial establishment of multiple connections is believed to serve the replacement of simpler interactions with more appropriate ones. The process of synaptic pruning takes place cell-specifically, at well-defined times and areas (Riccomagno and Kolodkin 2015). In general, it can fall into the following categories: stereotyped pruning, in which a neurite's faith is genetically predetermined and, therefore, can be predicted prior to its elimination or stabilization, and non-stereotyped pruning, in which limiting factors or neuronal activity define which neurites will be eliminated (Schuldiner and Yaron 2015). Neural activity influences pruning in the sense that long-term potentiation (LTP) or long-term depression (LTD) drive the maintenance or extinction of the synapse, respectively. LTP and LTD are two forms of activity-dependent neuroplasticity, that is the ability to alter the functional properties of neurons, in response to experience (Katz and Shatz 1996).
The main mechanisms that promote LTD are N-methyl-D aspartate receptor (NMDAR)-dependent and metabotropic glutamate receptors (mGluR)-dependent. When glutamate binds to the NMDAR, an increase of Ca^{2+} leads to kinase activation that in turn phosphorylates the GluR2 subunit of α-amino-3-hydroxy-5-methylisoxazole propionic acid receptor (AMPAR), resulting in endocytosis. This way, LTD is promoted by limited amounts of AMPAR in dendritic spines. Ca2+ influx also reduces AMPAR conductance via phosphorylation of the GluR1 subunit of AMPAR by protein phosphatase 1 (PP1) that is activated by active calcineurin. On the other hand, activation of group I mGluRs (mGluRI) leads to protein kinase C (PKC) activation that phosphorylates GluR2, thus enabling AMPAR elimination and LTD (Gladding, Fitzjohn, and Molnár 2009). Apart from NMDAR and mGluR-dependent LTD, alternative mechanisms can also account for neurite elimination, such as those involving semaphorins 7A and AB, (GABA)ergic inhibition, and the β-catenin/N-cadherin complex (Uesaka et al. 2014; Afroz et al. 2016; Bian et al. 2015).

A.3.2 Dendritic spines refinement

Synaptic pruning results from the retraction or degradation of axons and/or dendrites, which includes dendritic spine refinement (Riccomagno and Kolodkin 2015). Dendritic spines on pyramidal neurons are the sites where excitatory input is received and computed. During synaptogenesis, small membrane protrusions called filopodia arise from the dendrites' membrane (Portera Cailliau and Yuste 2001) and upon synaptic contact, they are transformed into spines (Portera-Cailliau, Pan, and Yuste 2003). Based on their morphology, dendritic spines can be divided into four main categories: mushroom (with a narrow neck and a large head), thin (with a narrow neck and a smaller head), stubby (with a large head and without any distinguishable neck), and cup-shaped (with two heads on top of a smaller neck) spines. Dendritic spines are typically less than 3 μm long: their heads have a diameter of 0,5-1,5 μm, while their necks' length is no more than 0,5μm long (Chidambaram et al. 2019). These spine morphologies are depicted in **Figure 2**. In the present study, we focus on stubby, mushroom, and thin spines. Mushroom and thin dendritic spines are more mature and stable structures compared to stubby spines and their generation largely depends on synaptic input and activity (Hotulainen and Hoogenraad 2010).

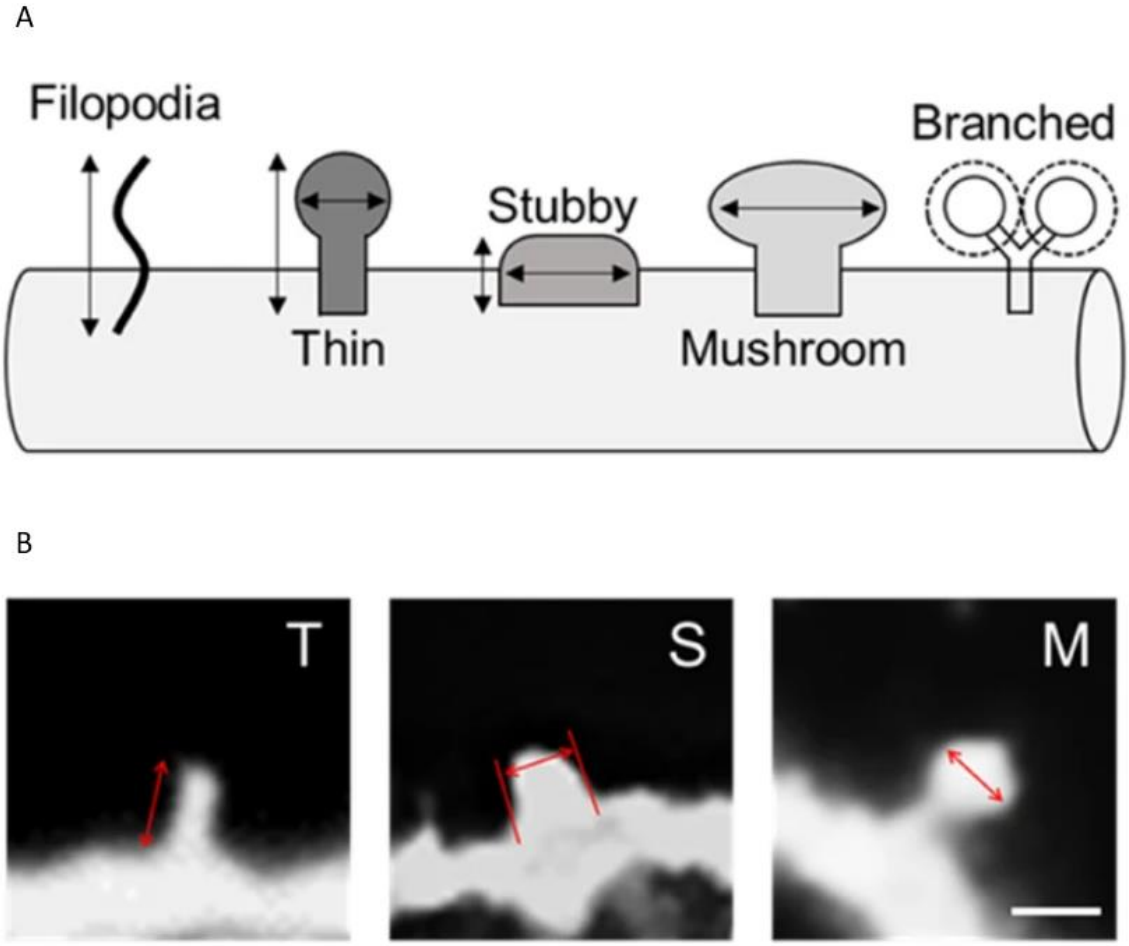

Figure 2: Types of membrane protrusions based on their morphology. (A) Illustration of the different types of spines. Filopodia are elongated membrane protrusions of 3-40 μm length. Thin dendritic spines consist of a thin neck connected to a small head. Stubby spines constitute spherical structures with no neck. Mushroom spines contain a narrow neck that ends up with a larger head, while cup-shaped or branched spines are characterized by two small heads attached to a shorter neck. **(B)** Images of thin (T), stubby (S), and mushroom (M) spines using two-dimensional light microscope. Figure adapted from (Chidambaram et al. 2019).

Dendritic spines are enriched in actin, cytoskeletal proteins, membrane receptors (AMPAR, NMDAR, metabotropic receptors), GTP-ase and interacting proteins, microRNAs, RNA-binding proteins, extracellular matrix, transcription factors, adhesion molecules, and post-synaptic density (PSD) regions. Glutamate binding to AMPAR or NMDAR leads to structural rearrangement of molecules like PDS-95, which in turn activates RhoGTPase or protein kinases signaling cascades. Synaptic strength and dendritic spine morphology are regulated by effectors like RhoA, Rnd1, Rac1, and Cdc42 (Chidambaram et al. 2019). Dendritic spines are dynamic structures, whose turnover is cell-type dependent, and potentially, brain region-specific. In particular, the apical dendrites of pyramidal neurons from cortical layers II, III exhibit higher turnover rates than those of pyramidal neurons from layer V (Holtmaat and Svoboda 2009).

LTD can result in dendritic spine shrinkage and loss (Becker et al. 2008; Simon Wiegert and Oertner 2013), however, biochemical evidence indicates that these two processes are underlined by different molecular pathways (Zhou, Homma, and Poo 2004; Wang, Yang, and Zhou 2007). Even though synaptic and spine plasticity can occur independently of one another (Sdrulla and Linden 2007),

spine plasticity that persists into adulthood contributes to the experience-dependent structural plasticity of neural circuits. These dynamical processes are promoted by redirecting synaptic strength (Holtmaat and Svoboda 2009), as depicted in **Figure 3**.

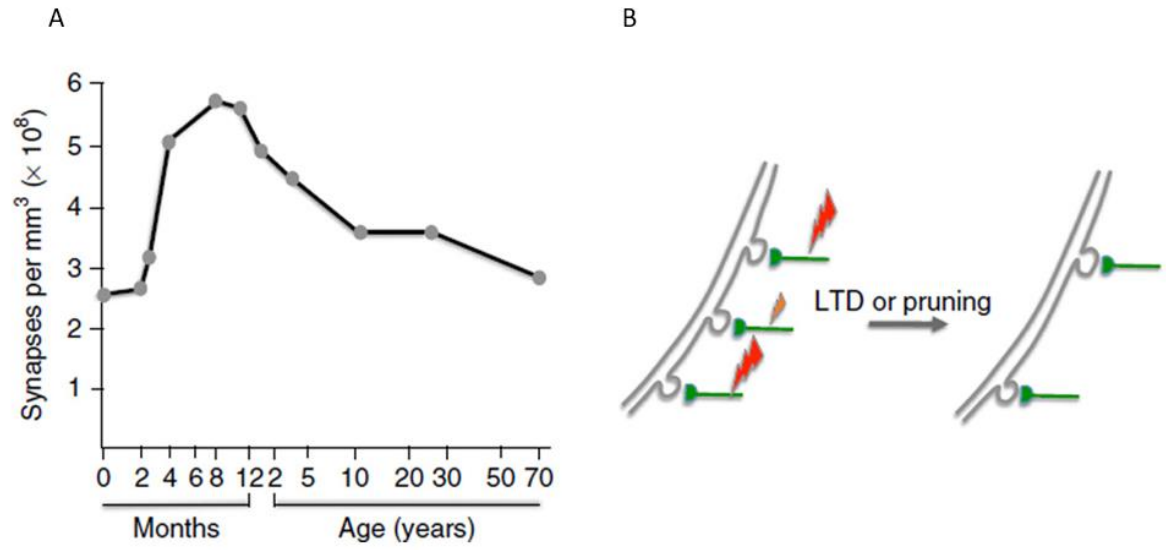

Figure 3: Experience-dependent synaptic pruning orchestrates the neural circuitry of the cortex. **(A)** Synaptic density in the human primary visual cortex, in respect to time. Note that the peak in synaptic density is reached in the first 2 years of postnatal life. **(B)** In the mammalian cortex, the levels of neural activity that dendritic spines receive define whether they will undergo stabilization or elimination. These processes are governed by plasticity rules (spine plasticity). Large and small lightning bolts represent increased or limited input strength to dendritic spines, respectively. LTD may result in spine elimination and synaptic pruning in weak synapses (Piochon, Kano, and Hansel 2016).

It is important to note that synaptic plasticity, in general, includes both the weakening or strengthening of preexisting synapses, as well as the synaptic elimination or *de novo* formation (Holtmaat and Svoboda 2009).

A.3.3 Cellular mechanisms and molecular control of pruning

Cellular mechanisms of pruning include local fragmentation or axon elimination by fragmentation, retraction, and axosome shedding. Fragmentation includes the generation of fragments after local caspase signaling that result in their destruction via the lysosome pathway. Glial cells that act as phagocytes seem to play a crucial role. Retraction refers to the reabsorption of axons or dendrites without the generation of fragments and underlies the degradation of smaller neural structures. Axosome shedding is a hybrid process that combines characteristics of both fragmentation and retraction. The axosomes, small pieces of retracting neurites that are left behind, are engulfed by glia and sent for lysosomal degradation. (Schuldiner and Yaron 2015). Characteristic examples of pruning by fragmentation include pyramidal neurons from layer V of the mammalian visual and motor areas (O'Leary and Koester 1993), as well as *Drosophila* mushroom body (MB) γ neurons (Technau and Heisenberg 1982). On the other hand, in mammals, granule cells in the hippocampus undergo pruning

by retraction (Bagri et al. 2003), and motor neurons undergo axonal shedding in order to establish proper neuromuscular junctions (Bishop et al. 2004).

Molecules that trigger the molecular mechanism of pruning include axon guidance receptors, receptors of the TGF-β family, and death receptors (Schuldiner and Yaron 2015). A schematic overview of the main molecules involved is shown in **Figure 4**.

Axon guidance receptor molecules mainly include semaphorins and ephrins, however, the relationship between their signaling is not clear yet. For instance, cortico-spinal connections of layer V visual cortex undergo pruning mediated by Neuropilin-2 (Nrp2) and Plexin-A (PlxA) complexes (Low et al. 2008). In particular, Semaphorin3F (sema3F) has been identified as an Nrp2/PlxA3 ligand in the hippocampus (Bagri et al. 2003), and it is speculated to guide also the pruning of layer V neurons of the visual cortex that interact with cortico-spinal connections (Low et al. 2008). Reverse ephrin signaling and more specifically, ephrin-B3 (EB3) signaling, is also implicated in hippocampal synaptic pruning (Xu and Henkemeyer 2009).

Pruning by TGF-β receptors has been mainly studied in *Drosophila* (Zheng et al. 2003), where a TGF-β ligand named Myoglianin (Myo) is secreted by neighboring glial cells (Awasaki et al. 2011). Plum, a protein belonging to the immunoglobulin superfamily, is believed to promote Myo availability to the receptor complex (Yu et al. 2013). The canonical TGF-β pathway requires dSMAD proteins and is regulated by the transcription of the steroid hormone Ecdysone Receptor-B1 (EcR-B1) (Zheng et al. 2003).

At this point, it is important to note that, in contrast to apoptosis, the neuron does not die when undergoing pruning (Maor-Nof and Yaron 2013). Nevertheless, in some neural systems, components of the apoptotic machinery are implicated in synaptic pruning. DR6/TNFSF21 and p75/ TNFRSF16 receptors, for example, both belonging to the TNF superfamily, account for efficient elimination of axons and dendrites in the PNS (Nikolaev et al. 2009; Singh et al. 2008).

Several proteolytic systems carry out the breakdown of axons and dendrites, such as those employing the ubiquitin-proteasome system (UPS), caspases, and calcium-activated calpains (Schuldiner and Yaron 2015) For instance, caspase-3 and caspase-9 activity are required for synaptic pruning in neurons of the sensory and sympathetic systems that have undergone trophic deprivation *in vitro (Cusack et al. 2013)*. In addition, downregulation and overexpression of calpastatin, an intrinsic inhibitor, enhanced and impeded pruning, respectively, both *in vitro* and *in vivo* in mice (J. Yang et al. 2013).

Many kinases are involved in the respective signaling pathways that lead to spine and eventually dendrite, or axon, elimination. GSK3α and GSK3β negatively regulate microtubule polymerization factors, thus affecting their stabilization and contributing to neurite degeneration (Chen et al. 2012). Kinases of the DLK-JNK pathway account for axon shrinkage in response to trophic deprivation (Ghosh et al. 2011), while there is evidence that the mammalian IκB kinase (IKK) also serves this role (Gerdts et al. 2011).

Synaptic pruning is practically mediated by disruption of the cytoskeleton, which is indicated by the above-described signaling pathways. Neurofilaments, microtubules, and actin are the main components of the cytoskeletal machinery. Neurofilaments provide structural support to axons, while actin promotes stabilization, as well as guidance throughout their assembly in neural circuits. Actin also stimulates axons to participate in the process of neuronal wiring. Microtubules are crucial for providing mechanical support and they contribute to organelle localization and intracellular trafficking (Schuldiner and Yaron 2015). In *Drosophila* and mammalian neuronal cultures, one of the first events that were observed during axonal pruning was the disruption of microtubules. In the case of cultured neurons, this destabilization was proved sufficient for axon fragmentation (Williams and Truman 2005; Luduena et al. 1986). Following trophic deprivation, paclitaxel, a microtubule-stabilizing agent, can prevent microtubules destruction and axon fragmentation. In mouse sensory axons, Kif2a, a

microtubule depolymerization kinesin, was found to facilitate microtubule breakdown upon fasting *in vitro* (Maor-Nof et al. 2013). On the other hand, actin regulates axon retraction. Indeed, Rac1, an important actin regulator, activity is inhibited during pruning in the mouse hippocampus and this inhibition is driven by the binding of the Sema3F receptor Neuropilin-2 to RacGAP β2-chimaerin (Riccomagno et al. 2012). Ephrin reverse signaling also regulates pruning of the hippocampal infrapyramidal bundle by binding to and activating the Grb-4 adaptor and the RacGEFDOCK180. This way, Rac1 gets activated (Xu and Henkemeyer 2009).

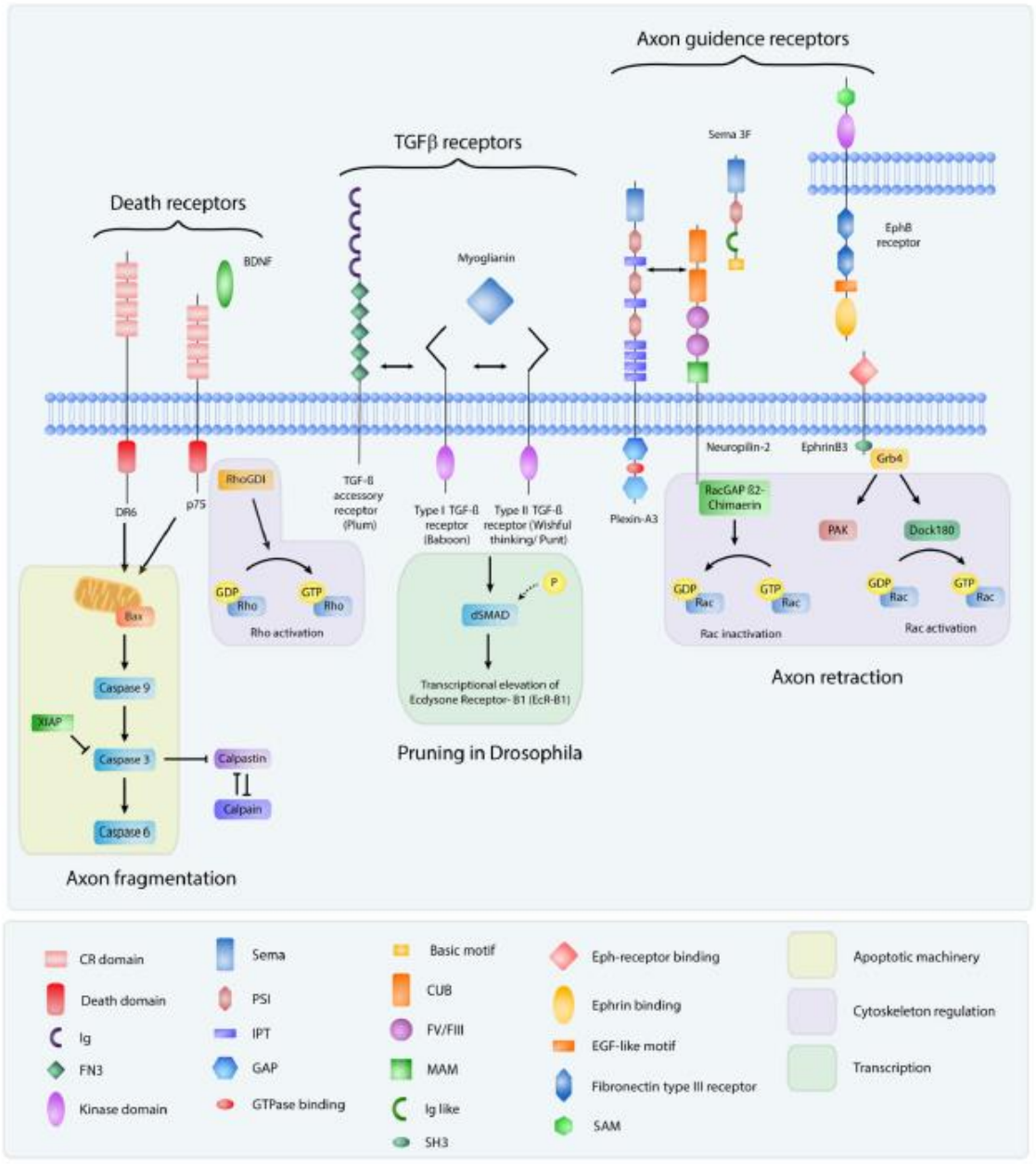

Figure 4: Schematic representation of the main molecules and mechanisms involved in the process of synaptic pruning. Axon guidance receptors, TGF-β receptors, and death receptors initiate the signaling cascades that result in cytoskeletal reorganization and eventually, axon or dendrite elimination, thus contributing to synaptic pruning (Schuldiner and Yaron 2015).

Axonal and dendritic pruning is also spatiotemporally regulated by the cell soma via the activation and effect of major transcription factors. As mentioned above, this process is regulated by EcR-B1 in Drosophila, whose targets include Sox14, MICAL, headcase, and Cullin1 (Kirilly et al. 2009; Loncle and Williams 2012). EcR-B1 expression is regulated by the cohesin complex, in post-mitotic neurons, nuclear receptor complexes, and the TGF-β signaling pathway (Schuldiner et al. 2008; Boulanger et al. 2010). In mammals, however, axonal and dendritic elimination occurs in the wider temporal windows of early postnatal life and puberty (Huttenlocher 1979).

There is a prominent role for glia in the clearance of fragments emerging from the process of synaptic elimination. In mammals, both astrocytes and microglia interfere with degenerating axons, as indicated with electron microscopy in the corpus callosum of cats (Berbel and Innocenti 1988). Schwann cells in the neuromuscular junction surround the retracting axons and engulf the remaining axosomes, which are then degraded by the lysosomes. (Bishop et al. 2004). In the hippocampus, as well as in the visual system, neuronal activity and expression of proteins of the complement system regulate microglia function in developing synapses (Schafer et al. 2012). In retinal ganglion cells of the dorsolateral geniculate nucleus of the thalamus, astrocytes participate in the process of pruning (Chung et al. 2013). Therefore, it becomes clear that synapse remodeling is, to a certain extent, mediated by processes that include substrate engulfment and degradation. These processes share common features with the broader concept of autophagy and further information on this term is given in the following section.

A.4 Autophagy

A.4.1 Definition and types of autophagy

Living cells need to receive molecules from their surrounding environment and at the same time, recycle their cytosolic components in order to maintain homeostasis. These processes are mainly mediated by membrane pieces that engulf the respective substrates and lead them to specific compartments for further processing. With neurons being post-mitotic, yet highly energy-demanding cells, proper regulation of their metabolism seems crucial for their survival. In eukaryotic cells, two major systems execute the degradation of unnecessary or damaged molecules: the lysosome and the proteasome. The proteasome exhibits high selectivity in its function, in the sense that it mainly recognizes ubiquitinated substrates. On the other hand, lysosome degradation is a more complex process. Autophagy is the predominant mechanism via which organelles and cytosolic components are delivered to lysosomes for degradation. Extracellular material and transmembrane proteins are delivered to lysosomes via the endocytic pathway (Mizushima and Komatsu 2011).

Autophagy can roughly be assigned to three main categories: macroautophagy, microautophagy and chaperone-mediated autophagy (Feng et al. 2014; Schuck 2020; Q. Yang, Wang, and Zhu 2019). Macroautophagy includes the enclosure of the substrate in an isolation membrane to form the autophagosome (also known as phagophore), which fuses with lysosomes, and in some cases, with endosomes (Feng et al. 2014). In microautophagy, the substrate is received directly by lysosomes (Schuck 2020). In chaperone-mediated autophagy, the chaperone protein Hsc70, along with other proteins, recognizes cytosolic proteins that carry the KFERQ-like signal and the complex is recognized by Lamp-2 located in the membrane of lysosomes (Q. Yang, Wang, and Zhu 2019). Macroautophagy is the most predominant type of autophagy and in the present study, we will refer to it as “autophagy”. Autophagosomes are usually formed in the endoplasmic reticulum (ER), however, recent studies show that the plasma membrane, the mitochondria, and the Golgi apparatus also promote autophagosome formation (Tooze and Yoshimori 2010). Genetic studies performed in yeast identified the so-called

autophagy-related genes (*ATG*), which are highly conserved among eukaryotes. In particular, Atg1-10, 12-14, 16, 17, 18, 29, and 31 are important for phagophore formation (Klionsky et al. 2003; Nakatogawa et al. 2009).

A.4.2 Molecular mechanism

The molecular mechanism of autophagy can be divided into distinct steps, which include initiation, vesicle nucleation, vesicle elongation, fusion with lysosomes, and degradation (Glick, Barth, and Macleod 2010). The mammalian target of rapamycin (mTOR), a serine-threonine kinase, regulates cell growth and survival, autophagy, and protein synthesis. Both presynaptic and postsynaptic sites contain mTOR, which is considered a negative regulator of autophagy (Laplante and Sabatini 2012). When activated, mTOR phosphorylates Unc-51-like autophagy-activating kinase 1 (ULK-1/Atg1) at S757, thus keeping ULK-1 away from AMP kinase (AMPK) and inhibiting autophagy (Jung et al. 2009). Autophagy can be induced by many stressors, such as limitation of growth factors, amino acids, oxygen, and energy. Other triggering factors might be endoplasmic reticulum stress, protein aggregation, or sensory deprivation. However, the initial induction of autophagy is rapid and precedes the total exhaustion of these resources (Kroemer, Mariño, and Levine 2010). The degradation products can be used for processes like energy synthesis, protein formation, gluconeogenesis, etc. Upon nutrients deprivation, cytoplasmic components are broken down via non-selective autophagy, whereas selective autophagy is mediated by the LC3-binding protein p62 (Mizushima and Komatsu 2011). Microtubule-associated protein 1A/1B-light chain 3 (LC3) is a soluble protein whose expression spans across many mammalian tissues. During autophagy, LC3-I, a cytosolic form of LC3, binds to phosphatidylethanolamine and creates LC3-phosphatidylethanolamine conjugate (LC3-II) which is then found in autophagosomal membranes. LC3-II recycling is permitted via degradation by lysosomes (Tanida, Ueno, and Kominami 2008). Selective autophagy can also be induced by stresses and is responsible for degrading specific proteins, organelles, and bacteria (Mizushima and Komatsu 2011).
Briefly, during initiation, AMPK phosphorylates ULK-1 at S137, rendering it active, in order for it to phosphorylate Beclin-1 at S14 (Russell et al. 2013). Activation of Beclin-1 is crucial for the process of vesicle nucleation, during which Endophilin 1 (ENDO1), an important transmembrane protein in presynaptic terminals, gets phosphorylated by LRRK2 kinase, thus inducing the generation of the isolation membrane and providing a binding site for Atg3. Elongation is characterized by the recruitment of LC3(Atg8), Atg16, and PI3K (Hwang, Yan, and Zukin 2019). Atg3 also transforms LC3-I to LC3-II, which interacts with the isolation membrane and drives elongation and enclosure of the cargo. The SAC1 domain of Synaptojanin-1 phosphatase also regulates autophagosome biogenesis by dephosphorylating PI(3)P/PI(3,5)P2 (Vanhauwaert et al. 2017). Mature autophagosomes carrying LC3-II are retrogradely transported from neuronal terminals to the soma, where they interact via p62 with lysosomes to form autolysosomes and degrade the cargo (Hwang, Yan, and Zukin 2019).

Autophagy can be regulated at the transcriptional level and epigenetically, with multiple ‘master regulators’ being implicated in these modification procedures (Füllgrabe, Klionsky, and Joseph 2014). In addition, brain-derived neurotrophic factor (BDNF), a key player in activity-dependent synaptic strength manipulation, has been found to repress autophagy in neurons of the adult brain (Nikoletopoulou et al. 2017). Bassoon, a protein that is important for the release of synaptic vesicles, binds to Atg5 and inhibits autophagy. Atg5 is an E3-like ligase that is activated by Atg7 and acts along with Atg12 and Atg16L1 to generate and arbor LC3II, thus contributing to isolation membrane extension and formation of the phagophore (Glick, Barth, and Macleod 2010). Atg16L1 is an Atg16-like protein found in autophagosomes (Okerlund et al. 2017). Although mostly studied at the presynaptic sites, autophagy at postsynaptic sites can also be induced, as in the case where GABAergic

signaling at the presynaptic terminal leads to sequestering of $GABA_A$ receptors inside autophagosomes (Rowland et al. 2006).

Besides recycling intracellular material, autophagy can also regulate neurotransmitter release through the interaction of autophagosomal Atg16L1 with Rab26, which is located in the membrane of synaptic vesicles (Binotti et al. 2015). Autophagy is associated with synaptic pruning, as indicated in a study where conditional ablation of atg7 in excitatory neurons resulted in aberrant pruning and increased spine density, along with autistic-like behaviors (Tang et al. 2014). Neuronal stimulation has been found to induce NMDAR-dependent autophagy via the PI3K-Akt-mTOR pathway, suggesting a role for autophagy in activity-dependent synaptic plasticity (Shehata et al. 2012). To this end, neuronal autophagy is believed to play a role in activity-dependent synaptic pruning by regulating synaptic activity, through receptor trafficking and maintaining synaptic vesicle homeostasis (Lieberman et al. 2019). Autophagy is also cell-autonomously required in pyramidal neurons for LTD-induction, which in turn triggers the local biogenesis of autophagic vesicles in dendrites (Kallergi et al. 2020). More information on dysregulated autophagy and synaptic pruning is given in the 'Pruning, autophagy and neurodevelopmental disorders sub-section'.

A.5 The Prefrontal Cortex (PFC)

In the present study, we focus on the prefrontal cortex (pfc). The prefrontal cortex can roughly be imagined as the cerebral cortex that extends to the front part of the frontal lobe. In all mammals, it receives projections from the mediodorsal nucleus of the thalamus, a key feature that reflects an identifiable group of actions. Its stimulation leads to no profound movements and in all primates, a granular layer IV is identifiable. All these facts have occasionally been used as criteria for its definition. Its increased size and functionality characterize more evolutionary complex organisms (Fuster 2002).

A.5.1 Structure and connectivity

Anatomically, the PFC can be divided into lateral, medial, and ventral or orbital aspects (Fuster 2002). Each prefrontal region can be also subdivided into distinct areas of well-defined cytoarchitecture (organization of cell bodies) and myeloarchitecture (architecture of myelinated fibers). Starting in the 20th century, many maps of the cerebral cortex were constructed, with the ones by Campbell (1905), Vogt (1906), Elliott Smith (1907), and Brodmann (1909) being the most famous ones. While the majority of the efforts focused on the human cortex, several ones aimed at reconstructing homologous regions in other species as well. In terms of cellular order architecture, the PFC exhibits the typical composition of the neocortex (the outer layer of telencephalon), which consists of six layers of cells, labeled from the outermost inwards, I to VI, as depicted in **Figure 5** (Palomero-Gallagher and Zilles 2019). More specifically:

Layer I or molecular layer: Few non-pyramidal neurons (Cajal-Retzius and spiny stellate cells) are found scattered in layer I, where also apical dendrites of pyramidal neurons from deeper layers end up. Horizontal axons from M-type thalamic neurons are also located (Cajal-Retzius area in **Figure 1**) in this layer (Rubio-Garrido et al. 2009), which receives input from the amygdala (Amaral and Price 1984) and other cortical regions as well (Vogt and Pandya 1978; Burkhalter and Bernardo 1989).

Layer II or external granular layer: Layer II receives input from many neocortical regions and consists of small pyramidal neurons and interneurons. Their axons end up at layer Vb, while their dendrites reach layer I (Palomero-Gallagher and Zilles 2019).

Layer III or external pyramidal layer: Cortico-cortical interactions mostly characterize layer III, which is subdivided into areas IIIa,b, and c. Many pyramidal neurons are found in this layer, with the ones of area IIIc being larger in size. However, non-pyramidal neurons are also present. The pyramidal neurons' dendrites of layer III extend up to layer I, while their horizontal axons reach layers II, IV, V, and VI. Apart from connecting with other-hierarchically either lower or upper- cortical areas, layer III also projects to the striatum (Palomero-Gallagher and Zilles 2019).
Layer IV or internal granular layer: Non primates lack a granular layer IV layer. In primates, however, spiny and aspiny stellate and pyramidal neurons reside in this layer. C-type thalamic neurons project there, where cortico-cortical afferents from the same hemisphere also end up. The pyramidal neurons' axons and dendrites reach layer I (Staiger et al. 2004).
Layer V or internal pyramidal layer: Layer V consists mostly of pyramidal neurons, whose differences in size and packing density account for the subdivision of this layer into areas Va and Vb. Many cortical and subcortical areas communicate with layer V, such as the thalamus, basal ganglia, and brain stem nuclei. The hick-tufted layer V pyramidal neuron is one of the most extensively studied neurons. The characteristic morphology of layer 5 pyramidal neurons consists of a pyramidal soma, out of which two dendrite domains emerge: the predominant apical dendrite and the basal dendrite. A single axon also sends collateral branches that ramify within the neocortex (Ramaswamy and Markram 2015). **Figure 6** illustrates an example of a pyramidal neuron.
Layer VI or the polymorphic layer: Several large pyramidal neurons and many smaller pyramidal, as well as non-pyramidal neurons, comprise layer VI. The more densely populated area of layer VI is known as VIa, whereas the area of lower cell density is called VIb. Layer VI also interacts with the thalamus, amygdala, and other cortical areas. The apical dendrites of layer VI extend up to areas IIIa/IIIb (Thomson 2010).

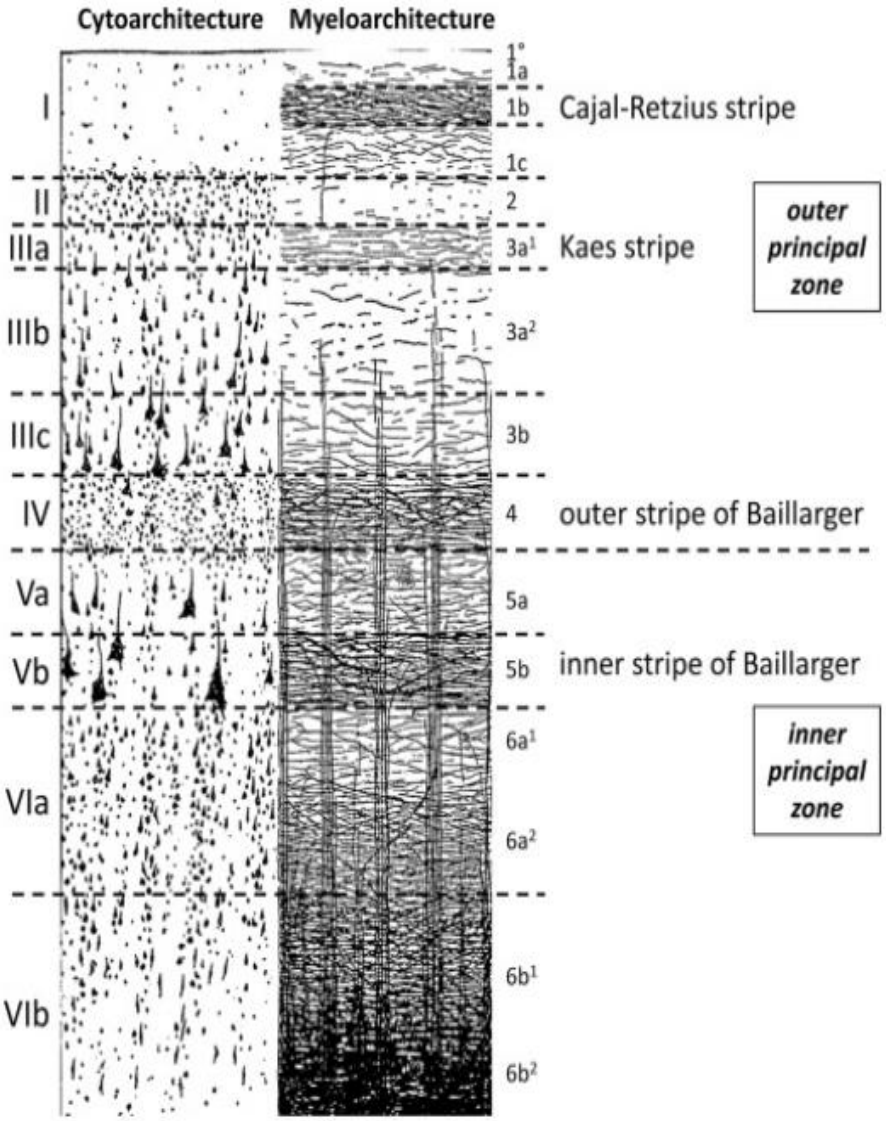

Figure 5: Representation of the characteristic neocortical layering that is present in the PFC. As depicted, the left part of the scheme refers to the organization of cell bodies (cytoarchitecture), while the right one refers to the organization of the myelinated axons (myeloarchitecture). *Note: The granular layer IV is absent from non-primates* (Palomero-Gallagher and Zilles 2019).

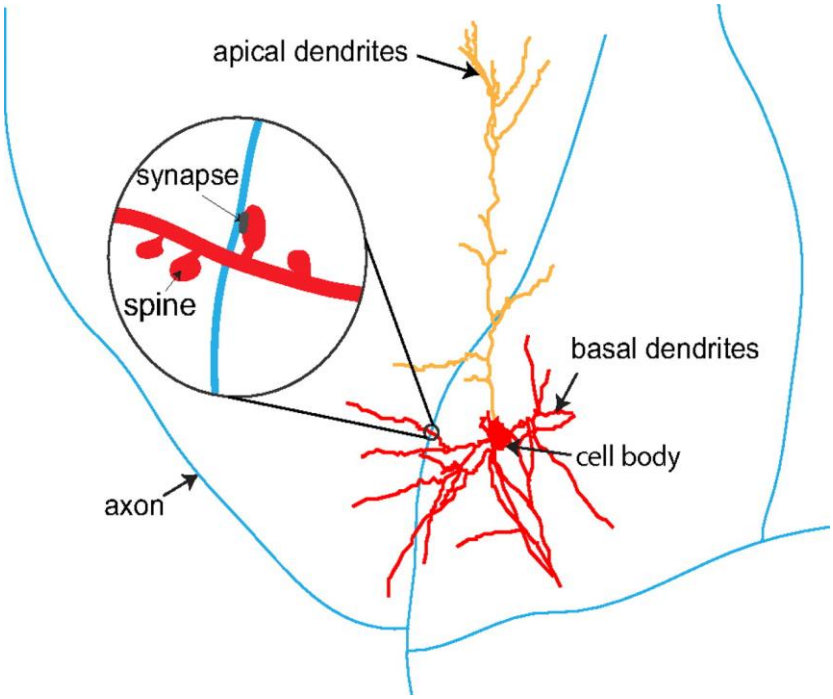

Figure 6: Schematic representation of the typical morphology of a pyramidal neuron. A basal dendritic tree (red) and an apical dendritic tree (orange) emerge from the cell soma. Dendritic spines typically indicate the sites of synapses between dendrites and axons (blue) of other neurons (Wen et al. 2009).

The human PFC can also be subdivided into two morphologically and functionally distinct regions: those of the ventromedial PFC (vmPFC)-consisting of the ventral and medial PFC-and the lateral prefrontal cortex (LPFC)-consisting of the dorsolateral and the ventrolateral regions. These two areas have followed different evolutionary paths, as the vmPFC is present in all mammals, whereas the LPFC is only found in primates (Striedter 2006). It is important to emphasize that the different layers and neuronal types of the cerebral cortex are widely considered to be functionally orchestrated in cortical columns and minicolums. These columns can be imagined as distinct modules of local neural circuits that are repeatedly found in each specific cortical area (Mountcastle 1997). The hypothesis was first introduced in the mid-'50s and was based on electrophysiological data from single-cell recordings of vertically oriented bands in the cat somatic cortex that revealed similar response properties (Mountcastle, 1957). Although the concept of smaller, repeated, and distinct units of neural circuitry representing the elementary units of cortical activity has driven brain research for many years, it remains debatable up to these days (Horton and Adams 2005).

A.5.2 Function and interconnections

The PFC is believed to contribute to the organization of cognitive, behavioral, and linguistic actions. Attention, working memory, and decision-making, all fall under the umbrella of cognitive actions. A term commonly used in the literature to include processes like these, represented by the PFC, is 'executive function'. A fundamental feature of executive function is that all of its underlying procedures contain a future perspective and aim towards the organization of goal-directed actions. Several aspects of attention are supported by all prefrontal cortical regions. However, the medial and anterior cingulate regions are associated with motivation, the lateral with working memory, and the orbital with inhibitory control of impulses and intervention (Carlén 2017).

The PFC exerts complexity in its connectivity with other brain areas, both cortical and subcortical. Of note, the nuclei of the anterior and dorsal thalamus interact with all prefrontal cortical regions, which are also interconnected with one another. The medial and orbital regions are connected with limbic structures like the hypothalamus, whereas the lateral region with basal ganglia and the association cortex. The connections between the PFC and the limbic structures account for the control of emotional behavior, while those between the PFC and the basal ganglia, for the coordination of motor behavior. In general, the early developing areas of the ventrolateral PFC support the expression and control of instincts and emotions, while the late-maturing areas of the ventral PFC are implicated in higher executive functions (Fuster 2002).

A.5.3 Development

Similar to other brain areas, the PFC exhibits the typical temporal sequence of developmental milestones. Neurons are generated and migrate to appropriate cerebral positions, mature, and form synapses, the majority of which are later on eliminated. The developing glia produces myelin and provides neurons with support and appropriate signaling. These important processes for human cortical development during gestation are shown in greater detail in **Figure 7** (Bryan Kolb et al. 2012). Fundamental procedures for the proper development of the PFC span from gestation until adulthood. This prolonged maturation of the PFC is believed to underlie the establishment of complex behaviors, which are shaped through interactions with the environment. Even innocuous experiences with no apparent consequences can have profound effects on prefrontal development. Indicative factors include maternal infection and malnutrition in prenatal life, and early stress, sensory and motor experience, parent-infant relations, peer relationships, and the use of psychoactive drugs in postnatal life and especially, in adolescence. Therefore, the prolonged maturation of the PFC compared to other cortical areas, as depicted in **Figure 8**, opens a long window of vulnerability to disruption (Selemon and Zecevic 2015; Bryan Kolb et al. 2012).

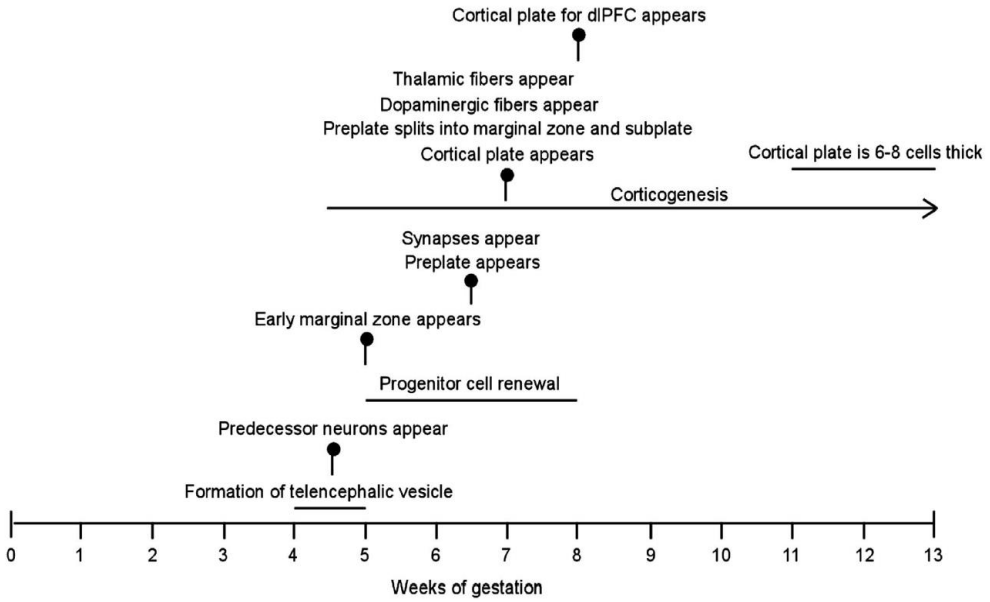

Figure 7: Developmental milestones for human cortical development during gestation. Note that corticogenesis begins around 4,5 weeks of gestation (Selemon and Zecevic 2015).

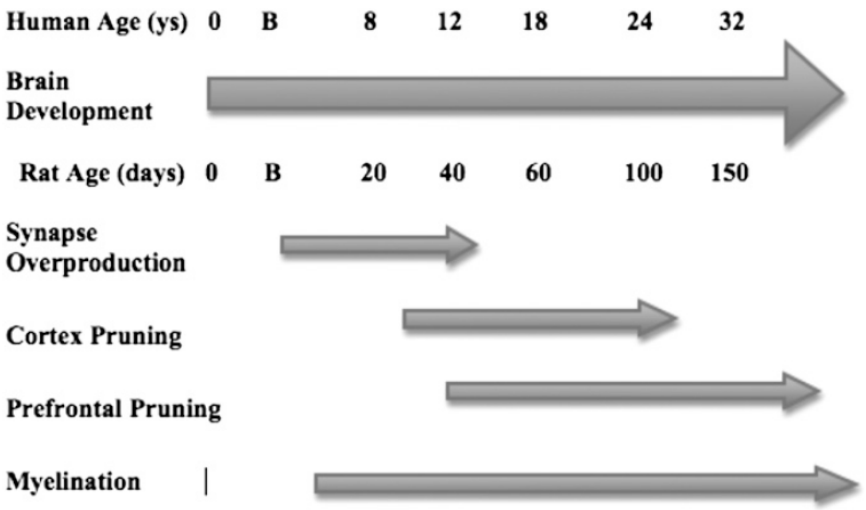

Figure 8: Timeline of brain postnatal development in humans and rodents. Note that the PFC development and in particular, synaptic pruning, exhibits a prolonged phase compared to other brain regions (Bryan Kolb et al. 2012).

A.6 The medial prefrontal cortex (mPFC)

Out of the three aspects of the PFC, here we focus on the medial PFC (mPFC). Rodents are widely used in brain research, as they constitute a genetically tractable system, whose manipulation and ethical considerations are simpler relative to human samples (Kaczmarczyk and Jackson 2015). As mentioned above, rodents do lack a granular layer IV and their PFC, on an anatomic basis, consists of the anterior cingulate cortex (ACC), the prelimbic cortex (PL), and the infralimbic cortex (IL) (Klune, Jin, and DeNardo 2021). In the present study, measurements were performed in the PL, which is shown in **Figure 9**.

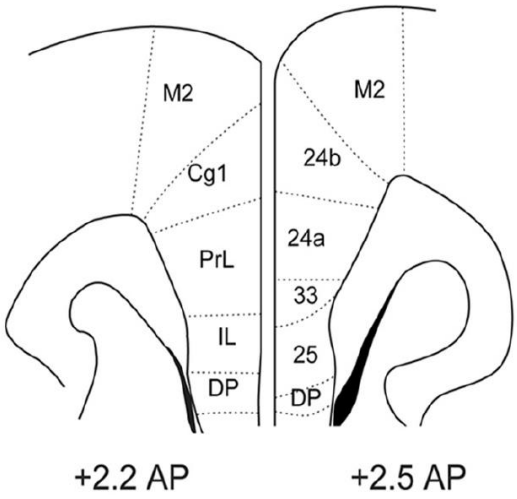

Figure 9: Anatomic basis of the rodent PFC. The rodent mPFC is represented by the ACC (its Cg1 subregion is shown here), the PL (here indicated as PrL), and the IL. The image is acquired from the 7th edition of the Paxinos and Watson rat brain atlas, where Brodmann's areas are also depicted (Laubach et al. 2018).

The rodents' postnatal life can be subdivided into the juvenile, adolescent, and adulthood periods. Despite small variations in their respective duration among different individuals and between sexes, the consensus is that the juvenile period spans the P0-P27, whereas adolescence and adulthood extend to P28-P48 and P49-P60, respectively. As described in the section above, through dynamical interactions with multiple brain areas or brainstem nuclei, mPFC supports several functions, out of which cognitive flexibility, working memory, and social behavior are of great importance for our study. During the juvenile period, augmented rates of synaptogenesis, as well as synaptic pruning, are observed in the mPFC. Also, neuronal excitability and synaptic strength are increased, while oscillations emerge through developing long-range interactions. Adolescence is generally considered a most critical time period, in the sense that exposure to novel stimuli, along with the robust hormonal changes that individuals undergo, can have long-lasting effects on the developing brain. During adolescence, rodents begin to create long-term fear memories, pursue goal-directed behaviors more effectively, and exhibit enhanced cognitive flexibility. Long-range connectivity strengthens, while local inhibitory neurotransmission initiates to develop. Synaptic pruning reaches its peak. Also, the monoamine neuromodulatory system and the endocannabinoid system start to develop (Klune, Jin, and DeNardo 2021). Elevated stress that commonly manifests during this time period has been shown to shift dopamine signaling in the mPFC towards excessive levels (Arnsten and Goldman-Rakic 1998). Given dopamine's prominent role in synaptic plasticity (Y.-Y. Huang et al. 2004), it comes naturally that its dysregulation promotes LTD via a long-lasting inhibition of LTP (Jay et al. 2004). This could result in

aberrant synaptic pruning. Dendritic spine density and neuromodulation undergo additional, milder changes during adulthood. (Klune, Jin, and DeNardo 2021). Several functionally important synaptic connections between the mPFC and other brain regions throughout development are shown in **Figure 10**.

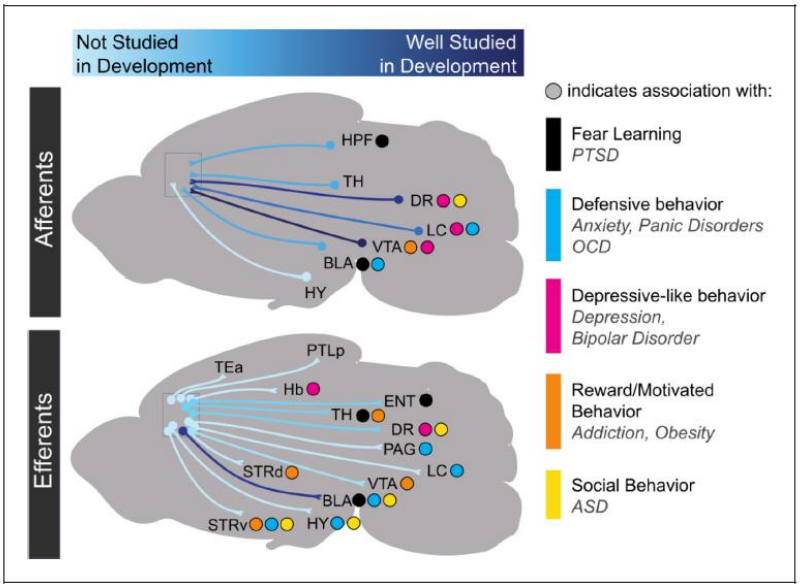

Figure 10: mPFC interconnections with other brain structures. Light blue projections represent poorly studied connections, whereas dark blue ones represent well-studied synapses. Disruption of these connections can result in disorders and associated behaviors, which are illustrated with dots of different colors. *HPF: hippocampal formation; TH: thalamus; DR: dorsal raphe nucleus; VTA: ventral tegmental area; LC: locus coeruleus; BLA: basolateral amygdala; HY: hypothalamus; TEa: temporal association area; PTLp: posterior parietal association area; Hb: habenula; ENT: entorhinal cortex; PAG: periaqueductal gray; STRd: dorsal striatum; STRv: ventral striatum (Klune, Jin, and DeNardo 2021).*

A.7 Pruning, autophagy and neurodevelopmental disorders

Certain studies associate deficient autophagy and synaptic pruning with neurodevelopmental diseases. Loss of mTOR-dependent autophagy underlies impaired synaptic elimination and leads to autistic-like behavior. Rapamycin, an mTOR complex 1 (mTORC1) inhibitor, restores deficient spine pruning in neocortical layer V neurons and social interactions in *Tsc2*$^{+/-}$ mice, but not in *Atg7*^{cKO} or *Tsc2*$^{+/-}$;*Atg7*^{cKO} double mutants (Tang et al. 2014). These data come in line with previous studies demonstrating that patients with autism-spectrum disorders (ASD) contain atypical structure and increased density of dendritic spines (Phillips and Pozzo-Miller 2015). CA1 hippocampal neurons of *Frm1* KO mice exhibit aberrant mTOR activity that leads to decreased autophagy and synaptic pruning. Knockdown of Raptor, an mTORC1 component, enhances mTORC1 signaling, activates autophagy, and restores spine density (Yan et al. 2018). mTORC1 and mTORC2 are two functional protein complexes of mTOR, which is negatively regulated by TSC1 and TSC2 (J. Huang et al. 2008). *Frm1* KO mice contain a mutation on the 5'-UTR of fragile X mental retardation 1 gene (*Fmr1*), resulting in hypermethylation and epigenetic silencing, thus causing Fragile x syndrome (Penagarikano, Mulle, and Warren 2007). Ablation of autophagy in microglia also impairs synaptic pruning and leads to the manifestation of social behaviors associated with ASD (Kim et al. 2017). *De novo* mutations in activity-dependent neuroprotective protein (ADNP) were identified in an ASD form and ADNP was shown to

promote autophagy in neurons (Sragovich, Merenlender-Wagner, and Gozes 2017). Indeed, whole-exome sequencing of data from patients with ASD has revealed small exonic copy number variations indicating dysregulated autophagy (Poultney et al. 2013). Last but not least, the neurodevelopmental hypothesis of schizophrenia suggests that impaired synaptic pruning in the PFC during adolescence accounts for the pathophysiology of the disease, and one can speculate that this could be mediated by decreased neuronal autophagy (Selemon and Zecevic 2015). Indeed, several autophagy-related proteins were found dysregulated in the brain and the periphery of patients with schizophrenia, including Beclin-1, Beclin-2, and ADNP. ADNP also co-precipitated with LC3II, suggesting a direct link between autophagy and the disease (Merenlender-Wagner et al. 2015).

B. Aim of the study

Autophagy is associated with the process of synaptic pruning and abnormal pruning underlies several neurodevelopmental diseases (Lieberman et al. 2019). In the present study, we aimed to examine the prefrontal cortical structure and function when neuronal autophagy is impaired during mouse adolescence, a critical period for PFC development. To this end, we used the Cre^{ERT2}-Tamoxifen system, which allows for spatiotemporal control of *Atg5* ablation, a gene important for phagophore elongation in autophagy. More detailed information on the way this system works is given in **Figure 11**. By performing selective breedings, we were able to generate the *thy1-*Cre^{ERT2}*;atg5*$^{f/f}$ conditional knockout, as well as the heterozygote *thy1-*Cre^{ERT2}*;atg5*$^{+/f}$, which exhibits milder autophagy impairment, and the genotype-related control animals. Tamoxifen administration was performed in adolescence or early adulthood (as a control). Behaviors that depend primarily on the function of the PFC (sociability-social memory, recency memory), as well as less-to our knowledge-depending on the PFC behaviors (novelty recognition memory, spatial memory), were tested with distinct behavioral experiments after animals had reached adulthood. Dendritic spine morphology and density of the PFC pyramidal neurons were studied under the optical microscope, after Golgi-cox staining.

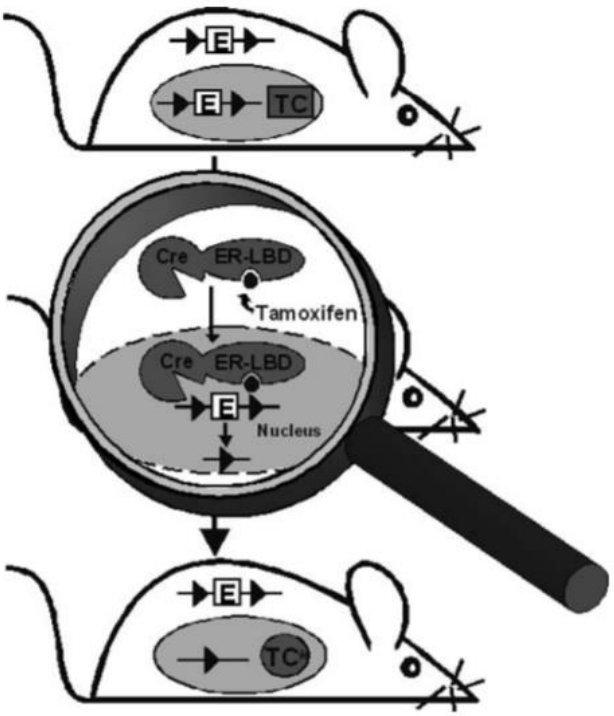

Figure 11: The Cre^{ERT2}-Tamoxifen system. In general, the Cre-Tamoxifen system promotes spatiotemporally controlled somatic mutagenesis based on the tissue-specific expression of the Cre recombinase. A loxP-flanked exon ('E' inside the square) inside the nucleus of the cells, in our case the *Atg5* gene, can be excised by a tamoxifen-dependent Cre recombinase ('TC'), in our case the tamoxifen-dependent Cre recombinase 2 (ERT2). The tamoxifen-dependent Cre recombinase is bound to a mutated ligand-binding domain (LBD) of the estrogen receptor (ER) and in the absence of tamoxifen, it is found in the cytoplasm ('TC' inside the square). Tamoxifen or OH binding to the LBD causes the Cre recombinase to translocate in the nucleus ('TC' inside the circle), where it can recombine the loxP-flanked piece of DNA (Feil, Valtcheva, and Feil 2009).

C. Methods & Materials

C.1 Animals

The animal protocols used for this study were approved by the FORTH Animal Ethics Committee (FEC). All experiments were conducted in adult animals (> 3 months old) of C57BL/6 genetic background. The mice were maintained in a pathogen-free environment and housed in same-sex groups of two up to five mice per cage, provided with standard mouse chow and fed *ad libitum*, under 12 hr/12hr light/dark cycle with constant temperature and humidity. *Atg5*$^{f/f}$ mice (Hara et al. 2006) were bred with *SLICK-H-Thy1-cre/*^{ERT2}*-EYFP* mice (The Jackson Laboratory strain 012708) to generate the *thy1-Cre*^{ERT2}*;atg5*$^{f/f}$ conditional knockout. Both genotype and the age at which tamoxifen (Tmx) was administered defined control groups. In *thy1-Cre*^{ERT2}*;atg5*$^{f/f}$ progeny and genotype-related control groups (*thy1-Cre*^{ERT2}*;atg5*$^{+/f}$, *thy1-Cre*^{ERT2}*;atg5*$^{+/+}$, *thy1-Cre*$^{ERT2(-)}$*;atg5*$^{f/f}$ *or thy1-Cre*$^{ERT2(-)}$*;atg5*$^{+/f}$ *or thy1-Cre*$^{ERT2(-)}$*;atg5*$^{+/+}$), tamoxifen was administered intraperitoneally at a dose of 75mg/kg bodyweight for 5 consecutive days, starting at P31 or P61. Control groups were injected intraperitoneally with the same volume of oil at the respective time period. Information on the abbreviations used in the present study for the animal groups is given in **Appendix A**. For the Three-Chamber Social Interaction task, 5 KO Tmx P30 (2 males, 3 females), 7 Het Tmx P30 (4 males, 3 females), 5 KO Tmx P60 (3 males, 2 females), 3 Het Tmx P60 (2 males, 1 female), 9 untreated (7 males, 2 females), and 10 genotype-related control with Tmx (5 males, 5 females) mice were used. For the Temporal Object Recognition task (TOR), 5 KO Tmx P30 (2 males, 3 females), 8 Het Tmx P30 (5 males, 3 females), 6 KO Tmx P60 (3 males, 2 females), 3 Het Tmx P60 (2 males, 1 female), 7 untreated (6 males, 1 female), and 7 genotype-related control with Tmx (3 males, 4 females) animals were used. For the Object-To-Place (OTP) task, 6 KO Tmx P30 (3 males, 3 females), 8 Het Tmx P30 (5 males, 3 females), 4 KO Tmx P60 (2 males, 2 females), 3 Het Tmx P60 (2 males, 1 female), 8 untreated (7 males, 1 female), and 10 genotype-related control with Tmx (5 males, 5 females) animals were used. For the Novel Object Recognition (NOR) task, 4 KO Tmx P30 (2 males, 2 females), 6 Het Tmx P30 (3 males, 3 females), 5 KO Tmx P60 (2 males, 3 females), 3 Het Tmx P60 (2 males, 1 female), 8 untreated (7 males, 1 female), and 9 genotype-related control with (5 males, 4 females) were used. Tamoxifen administration did not affect differentially the performance of male and female mice, as depicted in **Appendix B**.

C.2 Genotyping

DNA extraction was performed using chemical cell lysis on tail tissue derived from each animal. Each sample was incubated with 80μl of solution containing equal volumes of NaOH (50mM) and EDTA (0,4mM) for 1 hr at 95°C. Homogenous lysis was facilitated by vortex and spin-down of the samples every 20 min. The samples were finally neutralized using an equal volume of Tris-HCl (40mM, pH: 8) and stored at -20°C.

Wild type *Atg5* (*Atg5*$^{+}$) and *Atg5*^{flox} alleles, as well as *Thy1-Cre/*$^{ERT2(-)}$ and *Thy1-Cre/*^{ERT2} alleles, were detected with Polymerase Chain Reaction (PCR) and agarose gel electrophoresis. The oligonucleotides used are presented in **Table 1**.

Primers for the detection of *Atg5*$^{+}$ and *Atg5*^{flox} alleles		
NAME	SEQUENCE	SOURCE
Atg5(exon3-1)	5'-GAATATGAAGGCACACCCCTGAAATG-3'	Eurofins Genomics AT GmbH
Atg5(short2)	5'-GTACTGCATAATGGTTTAACTCTTGC-3'	Eurofins Genomics AT GmbH
Atg5(check2)	5'-ACAACGTCGAG CACAGCTGCGCAAGG-3'	Eurofins Genomics AT GmbH
Primers for the detection of *Thy1-Cre/*$^{ERT2(-)}$ and *Thy1-Cre/*^{ERT2} alleles		
NAME	SEQUENCE	SOURCE
Thy1-oIMR7303	5'-TCTGAGTGGCAAAGGACCTTAG-3'	Eurofins Genomics AT GmbH
Thy1-oIMR8744	5'-CAAATGTTGCTTGTCTGGTG-3'	Eurofins Genomics AT GmbH
Thy1-oIMR8745	5'-GTCAGTCGAGTGCACAGTTT-3'	Eurofins Genomics AT GmbH
Thy1-oIMR9296	5'-CGCTGAACTTGTGGCCGTTTACG-3'	Eurofins Genomics AT GmbH

Table 1: Primers for the detection of *Atg5*$^{+}$, *Atg5*^{flox}, *Thy1-Cre/*$^{ERT2(-)}$ and *Thy1-Cre/*^{ERT2} alleles.

The exact reagent quantities used for each Atg5 PCR reaction, as well as the program run by an MJR/Bio-Rad PTC-100 Programmable Thermal Controller, are shown in **Table 2** and **Table 3** respectively.

Atg5 PCR protocol			
COMPONENT	QUANTITY	WORKING CONCENTRATION	SOURCE
Genomic DNA	3 µl	-	Isolated from mouse tail tissue
PCR Buffer	2 µl	1X	Enzyquest
dNTPs	2 µl	2 mM	Enzyquest
Atg5(exon3-1) primer	0,6 µl	10 pmol/µl	Eurofins Genomics AT GmbH
Atg5(short2) primer	0,6 µl	10 pmol/µl	Eurofins Genomics AT GmbH
Atg5(check2) primer	0,6 µl	10 pmol/µl	Eurofins Genomics AT GmbH
Taq Polymerase	0,2 µl	5 u/µl	Enzyquest
Nanopure water	11 µl	-	-

Table 2: *Atg5* PCR protocol. Detailed information about the *Atg5* PCR components. PCR reactions were performed in a final volume of 20 µl. *Note: All reagents were stored at -20°C and the necessary manipulations were performed on ice.*

Atg5 PCR Program		
#STEP	TEMPERATURE	TIME
Step 1	94°C	180 sec
Step 2	94°C	30 sec
Step 3	60°C	30 sec

Step 4	72°C	60 sec
Step 5	Step 2, 30 times	
Step 6	72°C	360 sec
Step 7	4°C	Hold

Table 3: *Atg5* PCR Program. Detailed information about the *Atg5* PCR program run by an MJR/Bio-Rad PTC-100 Programmable Thermal Controller.

The exact reagent quantities used for each *Thy1* PCR reaction, as well as the program run by an MJR/Bio-Rad PTC-100 Programmable Thermal Controller, are shown in **Table 4** and **Table 5** respectively.

Thy1 PCR protocol			
COMPONENT	QUANTITY	WORKING CONCENTRATION	SOURCE
Genomic DNA	1,5 µl	-	Isolated from mouse tail tissue
PCR Buffer	2 µl	1X	Enzyquest
dNTPs	2 µl	2 mM	Enzyquest
Thy1-oIMR7303	1 µl	10 pmol/µl	Eurofins Genomics AT GmbH
Thy1-oIMR8744	1 µl	10 pmol/µl	Eurofins Genomics AT GmbH
Thy1-oIMR8745	1 µl	10 pmol/µl	Eurofins Genomics AT GmbH
Thy1-oIMR9296	1 µl	10 pmol/µl	Eurofins Genomics AT GmbH
DMSO	0,4 µl	2 %	Finnzymes

Taq Polymerase	0,16 µl	5 u/µl	Enzyquest
Nanopure water	9,94 µl	-	-

Table 4: *Thy1* PCR protocol. Detailed information about the *Thy1* PCR components. PCR reactions were performed in a final volume of 20 µl. *Note: All reagents were stored at -20°C and the necessary manipulations were performed on ice.*

Thy1 PCR Program		
#STEP	TEMPERATURE	TIME
Step 1	94°C	120 sec
Step 2	94°C	20 sec
Step 3	60°C	15 sec
Step 4	72°C	10 sec
Step 5	Step 2, 30 times	
Step 6	72°C	300 sec
Step 7	4°C	Hold

Table 5: Thy1 PCR program. Detailed information about the Thy1 PCR program. Note: All reactions were performed on an MJR/Bio-Rad PTC-100 Programmable Thermal Controller.

Atg5 PCR products were run on a 1% agarose gel, whereas *Thy1* PCR products were run on a 2% agarose gel, each one containing 2,5 µl of Ethidium Bromide (EtBr). Loading buffer 6X (containing Orange G and glycine) of 5 µl volume was added into each reaction and 23,5 µl of each sample were loaded into each gel well. The samples were run at 100 mV for 30 min and were then exposed to UV light for visualization.

C.3 Tamoxifen preparation

Tamoxifen (Sigma-Aldrich T5648) aliquots were prepared by dissolving tamoxifen in ethanol to a stock concentration of 100 mg/ml and they were stored at -20°C. One day prior to use, the solution was thawed and diluted in oil to a final concentration of 7,5 µg/µl. During all procedures, tamoxifen was protected from light exposure and its thawed form was kept at 4°C for no more than a week after its preparation, to avoid a decrease in its efficacy.

C.4 Behavioral experiments

Both male and female mice were injected intraperitoneally with tamoxifen or oil (control group) at P31 or P61 (control) for 5 consecutive days and were allowed to reach adulthood. Starting at P61 or P81 respectively, the animals were handled for 7 days, to get familiarized with the experimenter and thus, to reduce their stress levels. Then, their novel object recognition memory, spatial memory, and recency memory were tested with distinct Object Recognition tasks, whereas sociability and social memory were tested using a Three-Chamber Social Interaction testing paradigm. The temporal order of the behavioral experiments that mice underwent was the following: Novel Object Recognition task, Object-To-Place Recognition task, Temporal Order Recognition task, Three-Chamber Social Interaction task. The experimental outline is indicated in **Figure 12**.

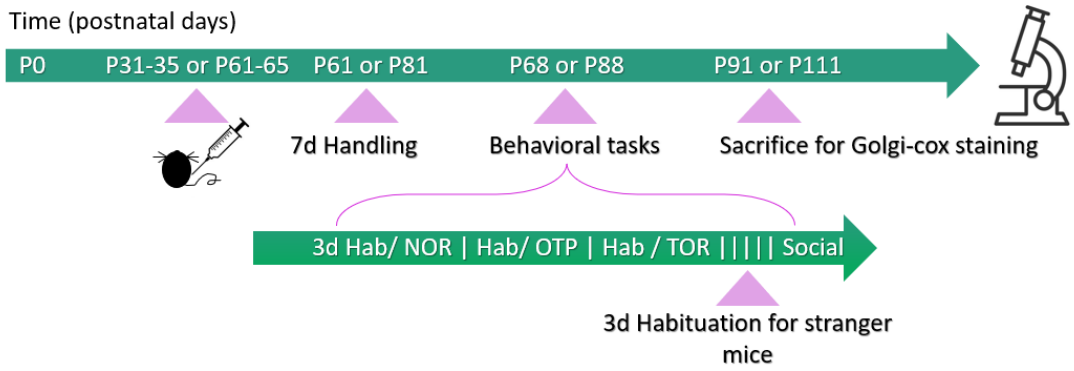

Figure 12: Experimental design. Mice of selected genotypes were treated with Tmx (75mg/kg) or oil at P31 or P61 (as a control) for 5 consecutive days. Starting at P61, or P81, respectively, they were handled for 1 week before the onset of the behavioral experiments. The temporal order of the behavioral experiments was the following: NOR, OTP, TOR, and Three-Chamber Social Interaction task. A 3-day series of habituation preceded the NOR task, whereas, for the OTP and TOR tasks, the habituation process was restricted to 1 day each. A break of a 1-day duration was allowed after completing each Object Recognition task and before the onset of the next habituation process. Between completing the TOR task and initiating the Three-Chamber Social Interaction task, a 5-day break was allowed, during which, a 3-day series of habituation of the stranger mice to the Three-Chamber Social Interaction apparatus was performed. Mice were left for 7-10 days to rest before they were sacrificed for Golgi-cox staining. *Note: Each vertical line (\) represents a break of a 1-day duration. 'Hab' stands for habituation and 'd' is a shortcut for day(s).*

C.4.1 Mouse Handling

After 1 hr of acclimation to the experimental room, mice were daily left to gradually explore the hands (gloves) of the experimenter for several minutes, until they were fully familiarized with the procedure. The handling lasted for approximately one week, with slight alterations in its duration customized to each mouse behavior. All manipulations were performed under normal light conditions, constant temperature, and humidity.

C.4 2 Novel Object Recognition task (NOR)

Once the handling procedure was completed, a 3-day series of habituation to the open-field apparatus followed prior to the day of the NOR task. For this purpose, mice were daily acclimated to the experimental room 1 hr prior to the habituation process with dim light, constant temperature, and humidity. Then, each mouse was placed in the center of a 45 x 45 x 45 cm open-field apparatus and was left for 15 min to explore it in the absence of the experimenter. The NOR task consisted of one sample trial followed by the test trial, after a 25 min break. Acclimation was also performed before the NOR task. In the sample trial, each mouse was placed in the center of the open-field apparatus facing two duplicates of one object (familiar object) and was left to explore them for 5 min. In the test trial, the mouse was placed again in the open-field apparatus, this time facing one familiar object from the trial phase and one novel object, and was left to explore them for 5 min. All objects were cleaned with 70% ethanol to remove any olfactory cues. Both the trial and the test phase were performed under low light conditions, in the absence of the experimenter and they were recorded. The time each mouse spent exploring the objects by physical proximity was the means by which object exploration, measured using JWatcher, was defined. The object exploration index was calculated as: [(novel object exploration time + familiar object exploration time) / total time in the open-field apparatus]. The discrimination index of the test trial was calculated as: [(novel object exploration time - familiar object exploration time) / (novel object exploration time + familiar object exploration time)].

C.4.3 Object-To-Place Recognition task

Once the NOR task was completed, mice were left to rest for a day, and then, they underwent habituation to the open-field apparatus for 15 min, after 1 hr of acclimation to the experimental room. The following day, the OTP task was performed, which consisted, similarly to the NOR task, of one sample trial and one test trial, separated by a 25 min delay. Acclimation was also performed before the OTP task. In the sample trial, each mouse was placed for 5 min in the center of the open-field apparatus facing two duplicates of one object, distinct from those of the NOR task, and was left to explore them. For the test trial, one object remained in the same location as in the trial phase (stationary object), whereas its duplicate was dislocated. The mouse was left to explore the objects for 5 min. All objects were cleaned with 70% ethanol to remove any olfactory cues. All procedures were performed in the absence of the experimenter and under dim light. The habituation process, as well as the trial and test phases, were recorded. The object exploration index was calculated as: [(displaced object exploration time + stationary object exploration time) / total time in the open-field apparatus]. The discrimination index of the test trial was calculated as: [(displaced object exploration time - stationary object exploration time) / (displaced object exploration time + stationary object exploration time)].

C.4.4 Temporal Order Object Recognition Task (TOR)

Once the OTP task was completed, mice were left to rest for a day, and then, they underwent habituation to the open-field apparatus for 15 min, after 1 hr of acclimation to the experimental room. The following day, the TOR task was performed. Acclimation was also performed before the TOR task. The TOR task comprised two sample trials followed by one test trial, all separated by 25 min delays. For the first sample trial (trial 1), each mouse was placed in the center of the open-field apparatus facing two duplicates of one object (old familiar object), distinct from those of the NOR and OTP tasks, and was left to explore them for 5 min. For the second sample trial (trial 2), the mouse was placed in the

center of the open-field apparatus facing two duplicates of a different object (recent familiar object) and was left to explore them for 5 min. For the test trial (test), the mouse was placed in the center of the open-field apparatus facing one object from trial 1 and one object from trial 2 and was left to explore them for 5 min. All objects were cleaned with 70% ethanol to remove any olfactory cues. All procedures were performed in the absence of the experimenter and under dim light. The habituation process, as well as the trial and test phases, were recorded. The object exploration index was calculated as: [(old familiar object exploration time + recent familiar object exploration time) / total time in the open-field apparatus]. The discrimination index of the test trial was calculated as: [(old familiar object exploration time - recent familiar object exploration time) / (old familiar object exploration time + recent familiar object exploration time)].

C.4.5 Three-Chamber Social Interaction task

The Three-Chamber Social Interaction task was performed approximately 5 days after the completion of the TOR task. The Three-Chamber Social Interaction task apparatus comprised one 60 x 40 x 22 cm (height) device consisting of three communicating compartments (chambers), 20 x 40 x 22 each. Free access to each chamber was allowed by small "door-like" openings. Before the experiment, C57BL/6 mice, newly introduced to the experimental mice ("stranger" mice), underwent 10 min daily habituations for 3 days into a cylindrical box with openings. The sociability test consisted of four successive phases. Firstly, each mouse was placed inside the middle compartment of the apparatus, with the openings closed, and was allowed a total time of 10 min to habituate. During phase I, the mouse was placed inside the middle chamber of the apparatus and was left for 10 min to habituate, this time being allowed to have free access to all compartments. During phase II, the mouse was placed in the middle chamber and was allowed to enter the other compartments, each of which contained one cylindrical box, with only one of them enclosing a stranger mouse of the same sex as the experimental mouse. The experimental mouse was left for 10 min to explore the whole device. The time of exploration was measured using JWatcher and the discrimination index was calculated as: [(stranger mouse exploration time - empty box exploration time) / (stranger mouse exploration time + empty box exploration time)]. During the social memory test (phase III of the sociability test), a new stranger mouse was introduced to the previously empty cylindrical box, apart from the stranger mouse of phase II (familiar stranger mouse), and the experimental mouse was placed inside the middle compartment and was left for 10 min to explore. The time of exploration was measured using JWatcher and the discrimination index was calculated as: [(new stranger mouse exploration time - familiar stranger mouse exploration time) / (new stranger mouse exploration time + familiar stranger mouse exploration time)].

Schematic representations of the three distinct Object Recognition tasks, as well as of the Three-Chamber Social Interaction task, are shown in **Figure 13** and **Figure 14**, respectively.

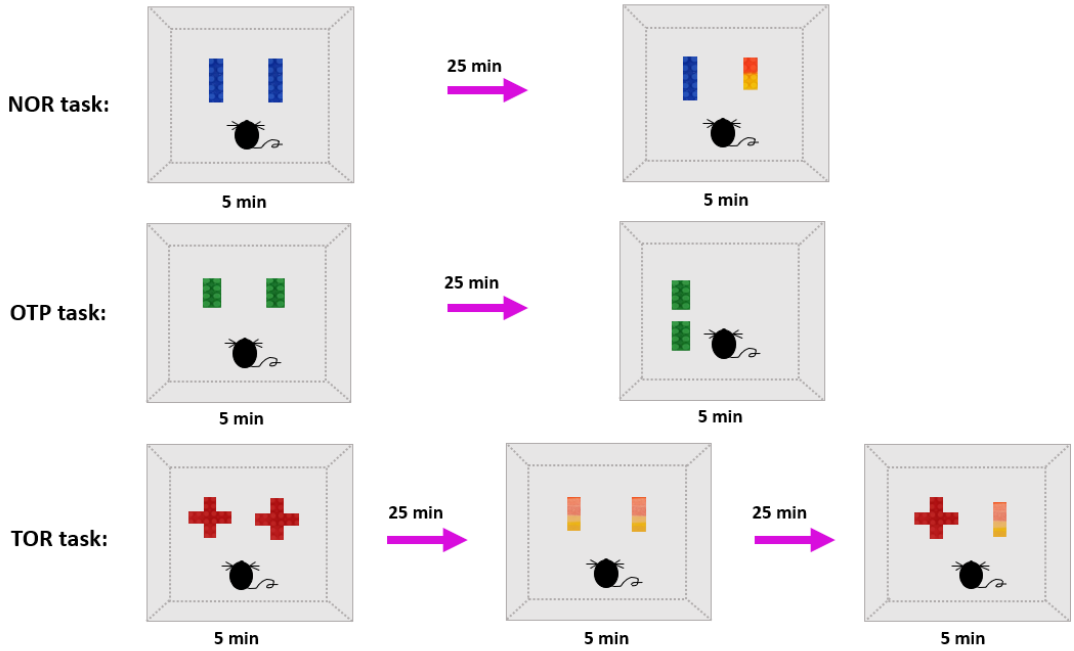

Figure 13: Graphical representation of the distinct Object Recognition (NOR, OTP, TOR) tasks.

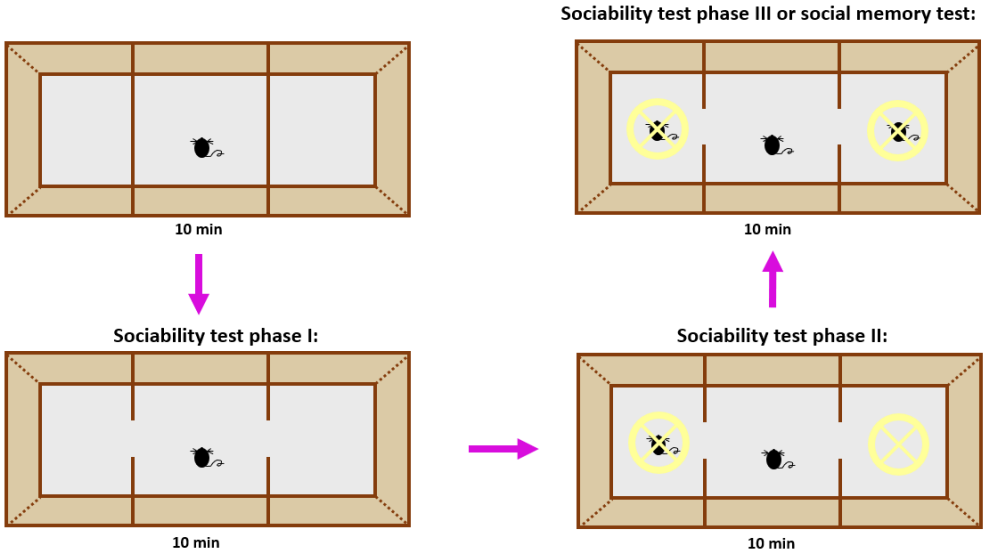

Figure 14: Graphical representation of the Three-Chamber Social Interaction task.

C.5 Statistical analysis

The data from the behavioral experiments were analyzed with t-test (for untreated animals and genotype-related control animals) and with one-way ANOVA (for KO TmxP30, Het Tmx P30, KO Tmx P60, and Het Tmx P60 animals). Statistically significant results from the ANOVA analysis were further interpreted with *post hoc* analysis (HSD).

C.6 Golgi-cox staining

The mice were sacrificed by spinal cord dislocation 7-10 days after completing the Three-Chambers Social Interaction task, and right after, their brains were removed. After being rinsed with distilled water, each brain was placed into a glass bottle containing 3-4 ml of Golgi-cox solution (5% Potassium Dichromate, 5% Mercuric Chloride (sublimate), and 5% Solution of Potassium Chromate), prepared at least 5 days earlier. Brains placed into the Golgi-cox solution remained in the dark at room temperature for 10 days and the solution was renewed every 2 days. On the 11th day, the brains were placed into a 30% sucrose solution and they were stored at 4°C. The brains were sliced in 150 μm - thick slices using a vibratome (Leica, VT1000S, Leica Biosystems GmbH, Wetzlar, Germany), and the slicing was performed in 6% sucrose solution. The brain slices containing the prelimbic area of the PFC (Bregma 2.96 mm - 1.54 mm) were placed onto microscope slides covered with parafilm and were maintained in a humidity chamber for approximately 30-40 hr at room temperature. After removing the parafilm, the slides were left for a few minutes in order for the slices to dry. Next, they were placed in distilled water for 1 min and were then incubated with Ammonium Hydroxide for 15 min. Another wash in distilled water for 1 min followed before the slides were incubated with Kodak Fix solution for 15 min. The slides were once again placed in distilled water for 1 min and were then dehydrated with increasing concentrations of ethanol (50%, 70%, 95%, 100%). A 3 min incubation in xylene followed prior to coverslip using Eukitt (Sigma-Aldrich 03989). The slides were kept in the dark for at least 2 months before imaging. All Golgi-cox manipulations were performed inside a laminar flow hood and, the steps of Ammonium Hydroxide and Kodak Fix incubations, in particular, were performed in the dark.

C.7 Optical microscopy

Dendritic spines of layer II/III and V pyramidal neurons in the prelimbic area of the prefrontal cortex were observed under the x60 lens of a Nikon Eclipse E800 Microscope. Approximately 2-3 pyramidal neurons per slice and 2-3 slices per animal were studied. Dendritic spines were assigned to the following categories: stubby, mushroom, and thin. Z - stacks were adjusted manually to obtain a valid perception of the total number of each spine subtype that was present in each dendrite segment. Mainly secondary and apical dendrites were observed and their spine densities were calculated. Image acquisition was performed using the Jenoptik ProgRes® CapturePro 2.8.8, whereas data analysis was performed in Microsoft Excel 2019.

D. Results

D.1 Generation of the appropriate mouse lines

By performing selective breedings, we were able to acquire the genotypes of interest: the conditional knockout, *thy1-Cre^{ERT2};atg5$^{f/f}$* (referred to it as KO), the heterozygote, *thy1-Cre^{ERT2};atg5$^{+/f}$* , (referred to it as Het), and the other genotype-related control groups that contain Cre^{ERT2} (*thy1-Cre^{ERT2};atg5$^{+/+}$), or not (thy1-Cre$^{ERT2(-)}$;atg5$^{f/f}$, thy1-Cre$^{ERT2(-)}$;atg5$^{+/f}$, thy1-Cre$^{ERT2(-)}$;atg5$^{+/+}$).* As depicted in **Figure 15**, the expected sizes for Atg5^{+}, Atg5^{flox}, *Thy1-Cre/$^{ERT2(-)}$*, and *Thy1-Cre/^{ERT2}* alleles were 350 bp, 750 bp, 341 bp, and 411 bp, respectively.

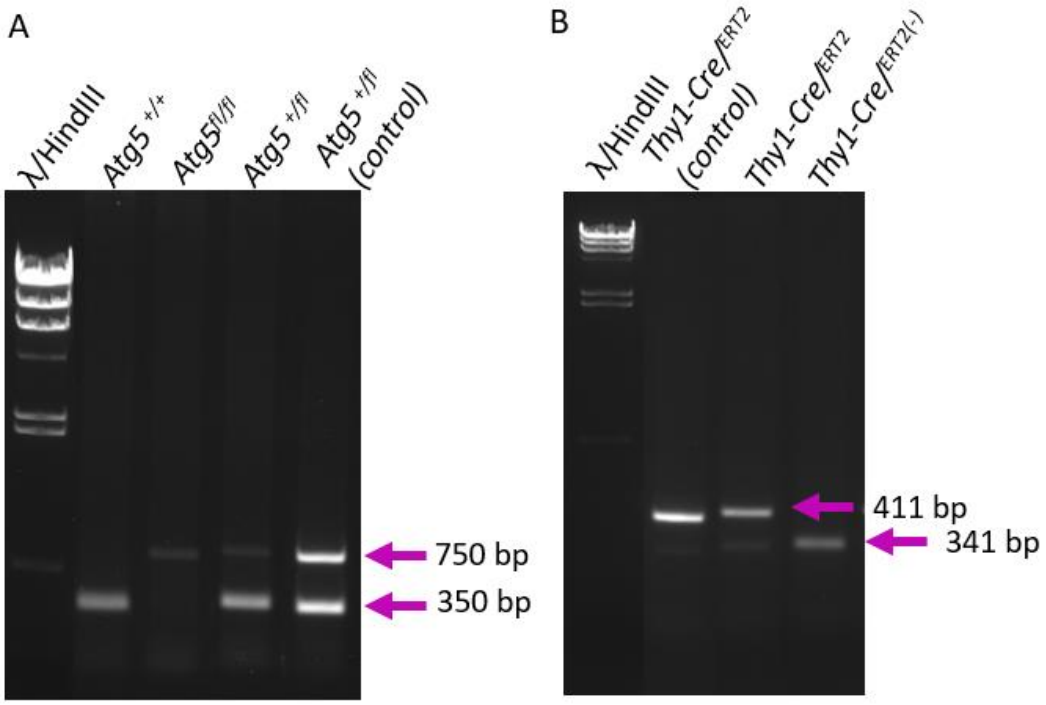

Figure 15: UV visualization of the different *Atg5* and *Thy1* alleles. (A) The *Atg5* PCR products were run on a 1% agarose gel. (B) The *Thy1* PCR products were run on a 2% agarose gel. *Red arrows indicate the size of the amplified DNA fragments.*

D.2 Effects of neuronal autophagy impairment on PFC spine density

Statistical analysis was not performed in spine density data, as the sample size in certain animal groups was limited, due to ongoing experiments. Therefore, more data is needed in order to draw reliable conclusions. However, some tendencies are worth noticing. Tamoxifen per se did not alter spine density, as the bars of control groups (no Tmx, genotype-related controls with Tmx) indicate (**Figure 16A**). The density of stubby spines seems to increase in KO Tmx P30 and Het Tmx P60 animals, compared to untreated and genotype-related control animals (**Figure 16**). Mushroom and thin spines constitute more mature structures compared to stubby spines and they exert prominent roles in synaptic plasticity (Pchitskaya and Bezprozvanny 2020). A tendency towards augmented densities of mature

spines is observed in all animals with impaired autophagy, either during adolescence or in early adulthood (KO Tmx P30, Het Tmx P30, KO Tmx P60, Het Tmx P60) (**Figure 16A**). Overall, we observe a tendency towards increased densities of mainly mature spines, in KO and Het animals, whose autophagy was impeded during adolescence or early adulthood.

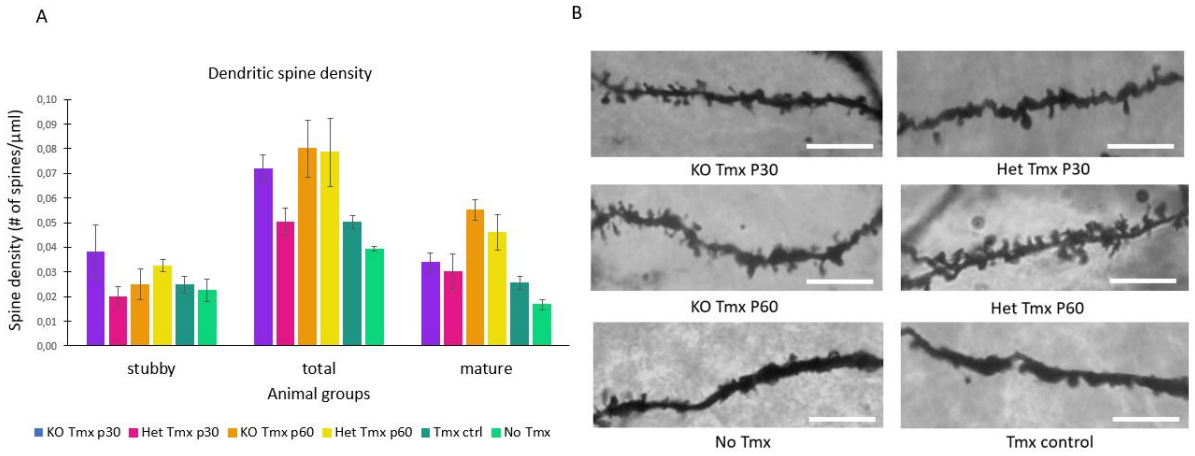

Figure 16: Neuronal autophagy impairment results in increased spine density of PFC pyramidal neurons. (A) Dendritic spine densities of each animal group. A tendency towards increased mature spine densities is observed in animals with impaired autophagy during adolescence or early adulthood. **(B)** Representative images were obtained with optical microscopy after Golgi-cox staining of PFC pyramidal neurons. *Scale bar: 10µm*

D.3 Effects of neuronal autophagy impairment on sociability and social memory

In phase II of the sociability task, untreated mice and genotype-related control mice administered with tamoxifen spent, on average, more time exploring the stranger mouse than with the empty cage, resulting in positive discrimination indices. Administration of tamoxifen did not lead to differences in the animals' performance (*t*-test, $p = 0.8764$) (**Figure 17A**). The distinct treatment groups (KO Tmx P30, Het Tmx P30, KO Tmx P60, Het Tmx P60) exhibited positive discrimination indices as well, with no significant differences among them, as one-way ANOVA analysis indicated ($F = 0.44975$, $p = 0.7203$) (**Figure 17A**). **Figure 17B** depicts the discrimination indices of individual animals from each group that participated in the sociability task. Tamoxifen, however, significantly increased the exploration index of genotype-related control mice compared to untreated mice (*t*-test, $p = 0.0159$), while autophagy impairment did not alter the exploration index of the distinct treatment groups ($F = 2.2333$, $p = 0.1174$) (**Figure 17C**). The exploration indices of individual animals participating in the sociability task are depicted in **Figure 17D**.

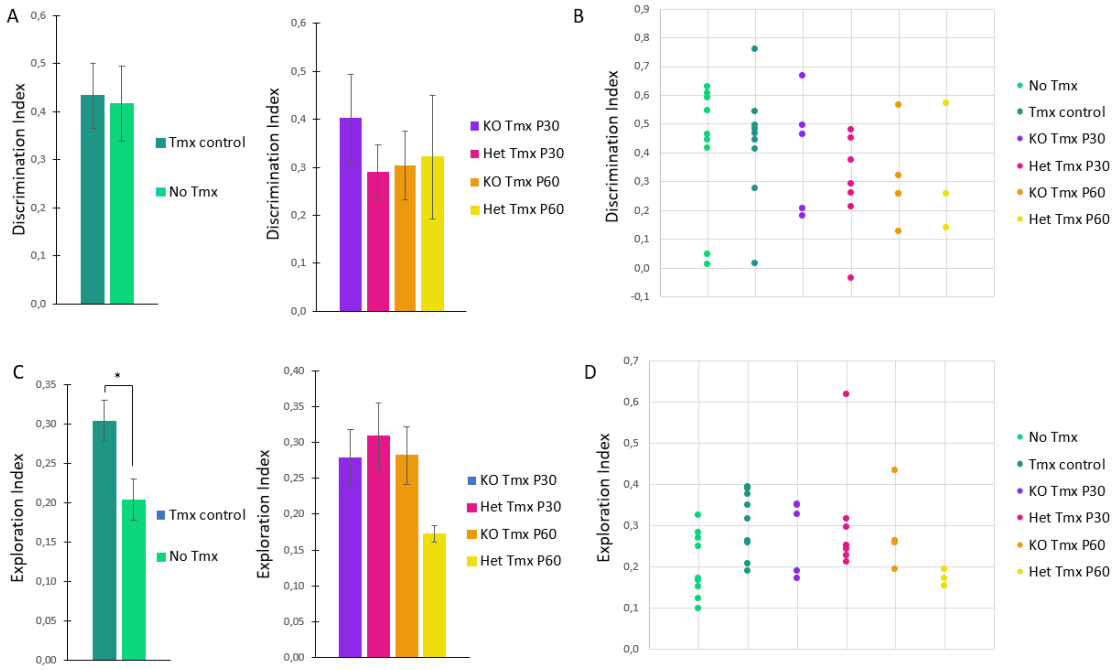

Figure 17: Neuronal autophagy impairment during adolescence does not affect sociability in mice. **(A)** *Left:* Discrimination index of control groups (no Tmx, genotype-related controls with Tmx) in the sociability task. Tamoxifen administration did not affect the animals' performance, as indicated with two-tailed *t*-test analysis (*t*-test, $p = 0.8764$). *Right:* Discrimination index of the distinct treatment groups (KO Tmx P30, Het Tmx P30, KO Tmx P60, Het Tmx P60) in the sociability task. One-way ANOVA did not reveal any statistically significant differences among the different groups ($F = 0.44975$, $p = 0.7203$). **(B)** Discrimination indices of individual animals participating in phase II of the sociability test. Each dot represents the discrimination index of each animal. Dots of the same color correspond to animals from the same group. **(C)** *Left:* Exploration index of control groups in the sociability task. Tamoxifen resulted in an increased exploration index, as revealed by two-tailed *t*-test analysis (*t*-test, $p = 0.0159$). *Right:* Discrimination index of the distinct treatment groups in the sociability task. No differences were observed ($F = 2.2333$, $p = 0.1174$). **(D)** Exploration indices of individual animals participating in the sociability test. $*p < 0.05$

Both untreated mice and genotype-related control mice treated with tamoxifen could discriminate between the novel and the familiar stranger mice from phases II and III of the sociability task, respectively, and spent more time exploring the less familiar stranger mouse, thus exhibiting positive discrimination indices. Not statistically significant differences were noticed (*t*-test, $p = 0.4411$) (**Figure 18A**). Heterozygotes and conditional knockout mice treated with tamoxifen during adolescence, as well as heterozygotes treated with tamoxifen at early adulthood also exhibited positive discrimination indices. However, this was not the case for conditional knockout mice, administered with tamoxifen during early adulthood, that exhibited decreased performance. Interestingly, these inconsistencies were not statistically significant ($F = 1.38848$, $p = 0.2768$) (**Figure 18A**). **Figure 18B** demonstrates the discrimination indices of individual mice that underwent the social memory test. Administration of tamoxifen did not alter the exploration index of genotype-related control mice (*t*-test, $p = 0.0243$) and autophagy impairment did not result in differences in the exploration index among the distinct treatment groups ($F = 1.15581$, $p = 0.3524$) (**Figure 18C**). **Figure 18D** shows the exploration indices of individual mice participating in the sociability test.

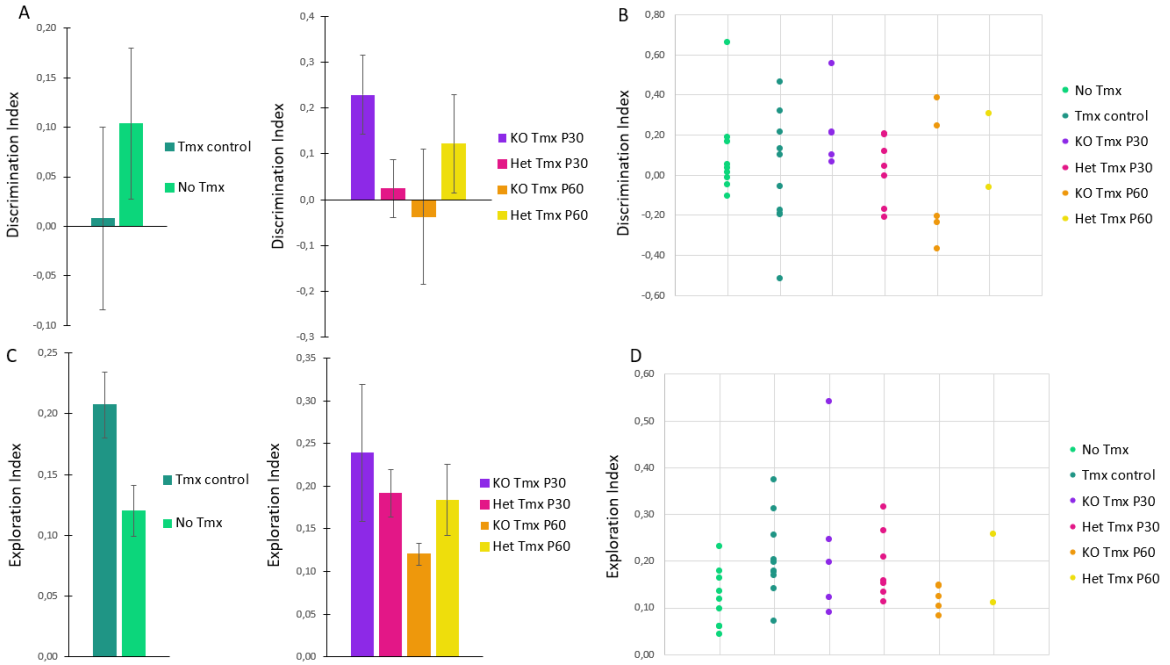

Figure 18: Neuronal autophagy impairment during adolescence does not affect social memory in mice. (A) *Left*: Discrimination index of control groups (no Tmx, genotype-related controls with Tmx) in the social memory test. No alternations in the discrimination index between control groups were observed (*t*-test, $p = 0.4411$). *Right:* Discrimination index of distinct treatment groups (KO Tmx P30, Het Tmx P30, KO Tmx P60, Het Tmx P60) in the social memory test. KO Tmx P60 exhibited a trend towards reduced performance, however, this trend was not statistically significant ($F = 1.38848$, $p = 0.2768$). **(B)** Discrimination indices of individual animals participating in the social memory test. Each dot represents the discrimination index of each animal. Dots of the same color correspond to animals from the same group. **(C)** *Left:* Exploration index of control groups in the social memory test. No differences were observed (*t*-test, $p = 0.0243$). *Right:* Exploration index of the distinct treatment groups in the social memory test. One-way ANOVA revealed no significant differences ($F = 1.15581$, $p = 0.3524$). **(D)** Exploration indices of individual animals participating in the sociability test. *$p < 0.05$

Overall, autophagy impairment during adolescence or early adulthood did not cause significant sociability and social memory deficits.

D.4 Effects of neuronal autophagy impairment on recency memory

In the test trial of the TOR task, untreated mice and genotype-related control mice treated with tamoxifen spent more time exploring the old familiar object compared to the recent familiar object, thus exhibiting positive discrimination indices that did not differ between these groups (*t*-test, $p = 0.4411$) (**Figure 19A**). However, One-way ANOVA analysis revealed inconsistencies in the performance among the distinct treatment groups ($F = 5.7175$, $p = 0.0050$). Heterozygotes treated with tamoxifen during adolescence, as well as conditional knockout mice and heterozygotes administered with tamoxifen during early adulthood, performed well. On the contrary, conditional knockout mice treated with tamoxifen during adolescence could not recognize the most recently presented object and spent less time exploring the less recently presented one. *Post hoc* analysis (HSD) identified a significant difference in the discrimination indices between KO Tmx P30 and Het Tmx P30 ($p = 0.0085$), KO Tmx P60 ($p = 0.0039$), and Het Tmx P60 mice ($p = 0.0376$), respectively (**Figure 19A**). **Figure 19B**

demonstrates the discrimination indices of individual mice that participated in the TOR task. Since tamoxifen administration did not result in different discrimination indices between genotype-related control mice treated with tamoxifen and their untreated littermates, the inconsistency that is observed in the distinct treatment groups' performance can be associated with impaired autophagy and not with tamoxifen's effects as a drug. Also, untreated mice and genotype-related control mice treated with tamoxifen did not exhibit differences in their exploration indices (*t*-test, $p = 0.4986$) (**Figure 19C**). One-way ANOVA analysis indicated that the distinct treatment groups did not exert important inconsistencies among their exploration indices as well ($F = 0.78731$, $p = 0.5144$) (**Figure 19C**). This suggests that the deteriorated performance of KO Tmx P30 mice reflects a defect in recency memory and is not a result of limited exploration attempts due to reduced motivation to explore. **Figure 19D** demonstrates the exploration indices of individual mice participating in the TOR task.

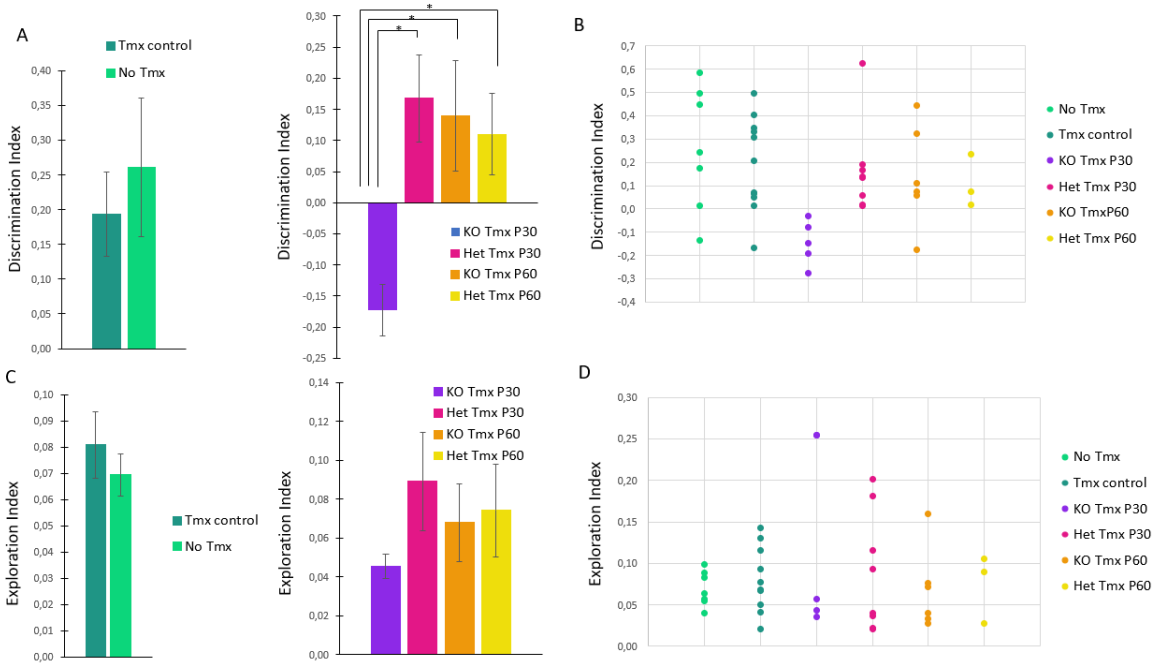

Figure 19: Neuronal autophagy impairment during adolescence results in impeded recency memory in mice. (A) *Left:* Discrimination index of control groups (no Tmx, genotype-related controls with Tmx) in the TOR task. Tamoxifen administration did not affect mice performance, as indicated with two-tailed t-test analysis (*t*-test, $p = 0.5484$). *Right:* Discrimination index of the distinct treatment groups (KO Tmx P30, Het Tmx P30, KO Tmx P60, Het Tmx P60). One-way ANOVA indicated a statistically significant difference of KO Tmx P30 mice compared to other treatment groups ($F = 5.7175$, $p = 0.0050$). **(B)** Discrimination indices of individual animals participating in the TOR task. Each dot represents the discrimination index of each animal. Dots of the same color correspond to animals from the same group. (C) *Left:* Exploration index of control groups in the TOR task. Not statistically significant differences were observed (*t*-test, $p = 0.4986$). *Right:* Exploration index of the distinct treatment groups. Not statistically significant differences were observed ($F = 0.78731$, $p = 0.5144$). (D). Exploration indices of individual animals participating in the sociability test. $*p < 0.05$

Therefore, we conclude that autophagy ablation from projection neurons during adolescence is associated with defects in recency memory.

D.5 Effects of neuronal autophagy impairment on spatial memory

In the OTP test trial, untreated mice and genotype-related control mice treated with tamoxifen exhibited positive discrimination indices that did not differ from one another (*t*-test, $p = 0.8081$) (**Figure 20A**). One-way ANOVA analysis showed differences in the performance of the distinct treatment groups ($F = 4.17276$, $p = 0.0198$). Heterozygotes administered with tamoxifen during adolescence exhibited a positive discrimination index in the OTP task. On the other hand, conditional knockout mice that had received tamoxifen during adolescence, as well as heterozygotes and conditional knockout mice treated with tamoxifen in early adulthood, could not discriminate between the stationary and the displaced object. *Post hoc* analysis identified a significant difference in the discrimination index of heterozygotes treated with tamoxifen during adolescence compared to that of heterozygotes treated with tamoxifen in early adulthood ($p = 0.0169$) (**Figure 20A**). Since tamoxifen administration did not lead to different discrimination indices between genotype-related control mice treated with tamoxifen and untreated mice, the poor performance of KO Tmx P30, KO Tmx P60, and Het Tmx P60 mice is a result of impaired autophagy and it cannot be associated with tamoxifen's effects. **Figure 20B** demonstrates the discrimination indices of individual mice that participated in the OTP task. In addition, untreated mice and genotype-related control mice treated with tamoxifen did not exhibit differences in their exploration indices (*t*-test, $p = 0.13054$) (**Figure 20C**). The distinct treatment groups did not exert important inconsistencies among their exploration indices as well ($F = 0.55967$, $p = 0.6474$) (**Figure 20C**). Again, this is indicative of spatial memory deficits in the case of KO Tmx P30, KO Tmx P60, and Het Tmx P60 mice, rather than of an artifact of limited exploration attempts due to reduced motivation to explore. **Figure 20D** demonstrates the exploration indices of individual mice that participated in the OTP task.

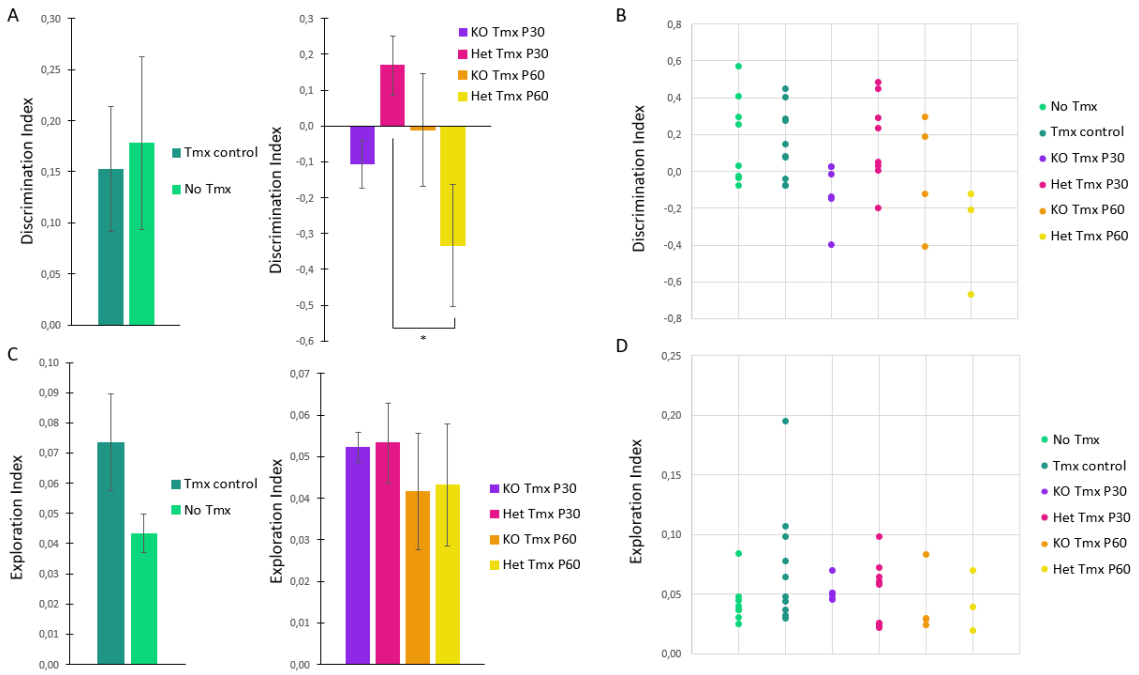

Figure 20: Neuronal autophagy impairment during early adulthood causes spatial memory deficits in mice. (A) *Left:* Discrimination index of control groups (no Tmx, genotype-related controls with Tmx) in the OTP task. Two-tailed t-test revealed no differences between control groups (*t*-test, $p = 0.8081$). *Right:* Discrimination index of the distinct treatment groups (KO Tmx P30, Het Tmx P30, KO Tmx P60, Het Tmx P60) in the OTP task. One-way ANOVA analysis revealed inconsistencies in the performance of the distinct treatment groups ($F = 4.17276$, $p = 0.0198$). KO Tmx P30, KO Tmx

P60, and Het Tmx P60 showed decreased performance, however, *post hoc* analysis (HSD) revealed that only Het Tmx P60 significantly differed from Het Tmx P30 ($p = 0.0169$). **(B)** Discrimination indices of individual animals participating in the OTP task. **(C)** *Left:* Exploration index of control groups in the OTP task. Not statistically significant differences were observed (*t*-test, $p = 0.13054$). *Right:* Exploration index of the distinct treatment groups in the OTP task. One-way ANOVA analysis revealed no significant differences among the groups ($F = 0.55967$, $p = 0.6474$). **(D)** Exploration indices of individual animals participating in the OTP task. *$p < 0.05$

Altogether, we demonstrate that neuronal autophagy impairment in early adulthood, but not in adolescence, is associated with spatial memory deficits.

D.6 Effects of neuronal autophagy impairment on novelty-recognition

In the NOR test trial, both untreated mice and genotype-related control mice treated with tamoxifen could discriminate between the novel and the familiar object, thus exhibiting positive discrimination indices that did not exert any differences (*t*-test, $p = 0.7975$) (**Figure 21A**). One-way ANOVA analysis revealed significant differences in the performance of the distinct treatment groups ($F = 6.32894$, $p = 0.0077$). Interestingly, conditional knockout mice treated with tamoxifen during adolescence performed poorly in the task, especially compared to conditional knockout mice ($p = 0.0065$) and heterozygotes ($p = 0.0140$) that had received tamoxifen in early adulthood, as *post hoc* analysis revealed (**Figure 21A**). Since tamoxifen administration did not lead to different discrimination indices between genotype-related control mice treated with tamoxifen and untreated mice, the decreased performance in the NOR task observed in KO Tmx P30 mice can be attributed to autophagy ablation during adolescence and is not associated with tamoxifen's effects. **Figure 21B** demonstrates the discrimination indices of individual mice that participated in the NOR task. Untreated mice and genotype-related control mice treated with tamoxifen did not exhibit differences in their exploration indices (*t*-test, $p = 0.5340$), and neither did the distinct treatment groups ($F = 0.2455$, $p = 0.8634$). Therefore, the reduced performance of conditional knockout mice, that were administered with tamoxifen during adolescence, in the NOR task is indicative of a defect in novelty-recognition and is not a result of limited exploration attempts due to reduced motivation to explore.

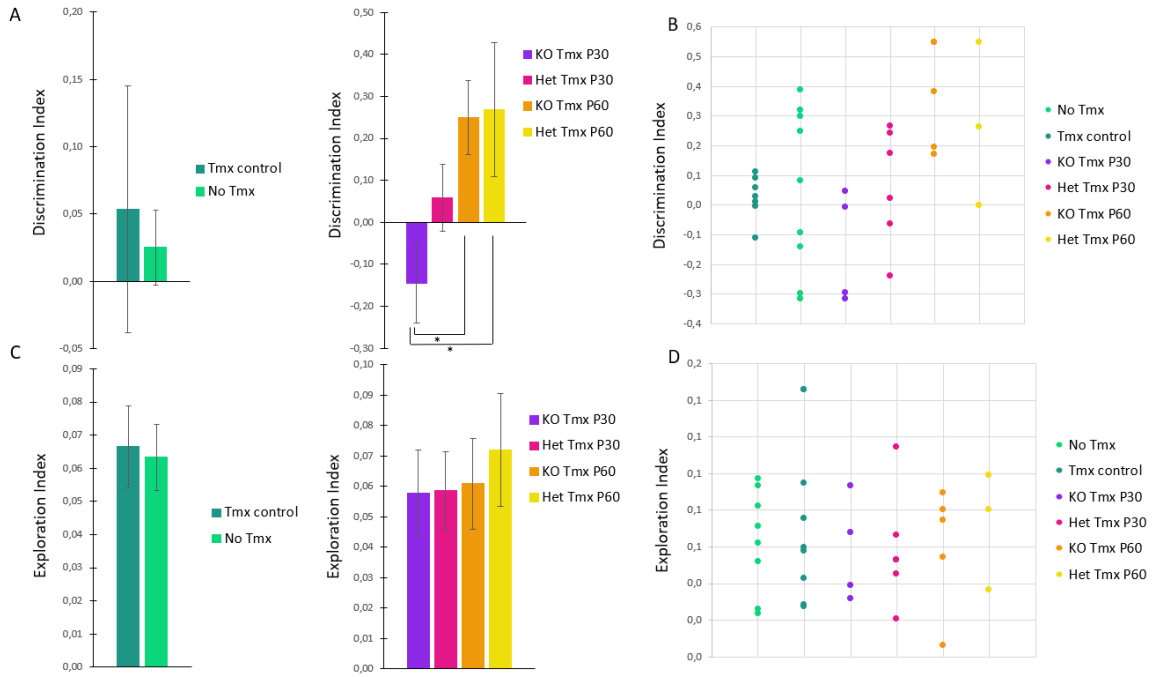

Figure 21: Autophagy ablation during adolescence affects novelty-recognition in mice. (A) *Left:* Discrimination index of control groups (no Tmx, genotype-related controls with Tmx) in the NOR task. No differences were observed (*t*-test, $p = 0.7975$). *Right:* Discrimination index of the distinct treatment groups (KO Tmx P30, Het Tmx P30, KO Tmx P60, Het Tmx P60) in the NOR task. One-way ANOVA analysis revealed inconsistencies in the performance of the distinct treatment groups ($F = 6.32894$, $p = 0.0077$). *Post hoc* analysis (HSD) indicated a decreased performance of KO Tmx P30 compared to KO Tmx P60 ($p = 0.0065$) and Het Tmx P60 ($p = 0.0140$) mice. **(B)** Discrimination indices of individual mice participating in the NOR task. **(C)** *Left:* Exploration index of the control groups in the NOR task. No differences were observed (*t*-test, $p = 0.5340$). *Right:* Exploration index of the distinct treatment groups in the NOR task. One-way ANOVA analysis revealed no differences among the groups ($F = 0.2455$, $p = 0.8634$). **(D)** Exploration indices of individual mice participating in the NOR task. $*p < 0.05$

In conclusion, we notice that autophagy impairment in projection neurons during adolescence is followed by defects in novelty-recognition.

E. Discussion

Pruning is a fundamental neurodevelopmental process that includes the elimination of dendritic spines to result in synapse reorganization. Autophagy is implicated in this process, with its underlying mechanisms of action being elusive. Defective pruning manifests in several neurodevelopmental diseases, therefore, understanding the association between pruning and autophagy is of major importance (Lieberman et al. 2019). In this study, we aimed to understand how prefrontal cortical development, and more specifically the process of synaptic pruning, is affected when autophagy is impaired during adolescence. To this end, we used the Cre^{ERT2}-Tamoxifen system to genetically ablate *Atg5*, a gene important for the process of autophagy, from projection neurons during mouse adolescence (around P30) and, as a control, in early adulthood (around P60). Cre^{ERT2}-recombinase activity is not detected in oligodendrocytes, astrocytes, or non-neural cells in *SLICK-H-Thy1-cre/^{ERT2}-EYFP* animals and, therefore, autophagy impairment in the *thy1-Cre^{ERT2};atg5$^{f/f}$* conditional knockout is strictly restricted in projection neurons of the CNS and PNS. It is widely accepted that pruning in the mPFC occurs between P31 and P42 (Shapiro et al. 2017), therefore, autophagy ablation starting at P35, when tamoxifen injections are completed, coincides with the process of synaptic pruning in this brain area.

E.1 Spine density in response to neuronal autophagy impairment

To determine how prefrontal cortical structure is altered in response to autophagy impairment, we performed Golgi-cox staining, a method traditionally used to study neurons' morphology (Zaqout and Kaindl 2016), in brain slices containing the PFC from mice that had received tamoxifen or oil (as a control) during adolescence or early adulthood (as a control). Tamoxifen administration per se did not cause any significant alterations in spine density, as preliminary data indicate (**Figure 16A**). However, a trend towards increased spine densities compared to control groups (untreated and genotype-related control mice treated with tamoxifen), in particular for mature spines, was observed in all animal groups with impeded autophagy (KO Tmx P30, Het Tmx P30, KO Tmx P60, Het Tmx P60). Interestingly, increased spine densities observed in mice with impaired autophagy during early adulthood (KO Tmx P60, Het Tmx P60) are in agreement with previous work performed in the lab (**Figure 21**), in which, dendrites from pyramidal neurons of male C57BL/6 mice were observed with optical microscopy after Golgi-cox staining in different ages. As expected, spine density follows a decline between P30-P50, in all spine morphologies of both apical and secondary dendrites and this temporally coincides with synaptic pruning in the mPFC (Shapiro et al. 2017). To our surprise, the density of mushroom spines in both apical and secondary dendrites was found to decrease, starting at P60. Also, in secondary dendrites, thin spine density at P90 did not significantly differ from that of P60, but it dramatically declined around P120 (**Figure 21**). We hypothesize that a second wave of spine and hence, synaptic elimination, might take place in the PFC during early adulthood. It is widely accepted that synaptic pruning sculpts prefrontal neural circuitry during adolescence. Only a few mentions are present in the literature on the existence of later-maturing synapses in the PFC. These so-called "late-blooming" synapses form when the majority of the PFC undergoes synaptic pruning, suggesting that their maturation takes place later on. Reciprocal connections of both the BLA and the ventral tegmental area (VTA) with the mPFC fall into this category (Delevich, Thomas, and Wilbrecht 2018). However, late maturation of synapses that orchestrate mPFC intra-connectivity and their association with prolonged synaptic pruning has not been reported. More work needs to be done in order to shed light on this potential, novel synaptic pruning activity. Future experiments focus on impairing autophagy after P60 and studying PFC integrity. In any

case, our findings indicate a direct link between autophagy and synaptic pruning that manifests in the level of spine elimination.

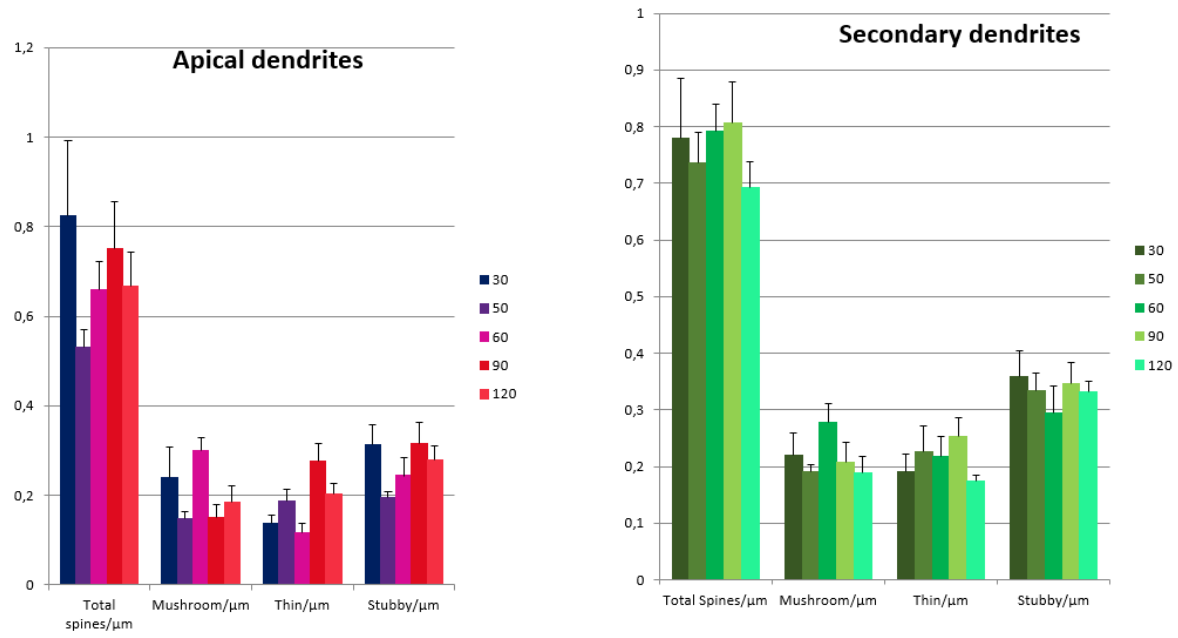

Figure 21: Dendritic spine densities in the PFC across different ages. Preliminary data from previous work in the lab identifying a decrease in mushroom spine density starting at P60 in both apical and secondary dendrites and a decrease in thin spine density starting at P60 in secondary dendrites.

Overall, there is a trend towards reduced spine densities at P120 compared to those observed at P60, suggesting that another wave of spine elimination in the PFC, distinct from that occurring during adolescence, might exist as well. These data resulted from Golgi-cox staining of brain slices derived from animals of different ages (P30, P50, P60, P90, P120).

E.2 PFC function after neuronal autophagy impairment

Higher cognitive functions that are mainly supported by the PFC were studied with distinct behavioral experiments. For sociability and social memory testing, a Three-Chamber Social Interaction paradigm was adapted. The PFC has a prominent role in social cognition (Bicks et al. 2015), therefore we postulated that impairing the normal PFC development and in particular the process of synaptic pruning, would result in severe social behavior deficits. Tamoxifen administration did not affect the ability to discriminate between the stranger mouse and the empty cage and autophagy impairment did not prevent mice from exploring the stranger mouse more than with the empty cage (**Figure 17A**). However, tamoxifen administration resulted in an increased exploration index in the genotype-related control group compared to untreated littermates, while it did not cause any inconsistencies in the discrimination index among the distinct treatment groups (KO Tmx P30, Het TmxP30, KO Tmx P60, Het Tmx P60) (**Figure 17 C**). More animals performing the experiment would inform us about whether this trend is for real, or if it is an artifact of the limited sample size. In the social memory test, tamoxifen administration did not result in differences in the discrimination index between untreated mice and genotype-related control animals administered with tamoxifen, therefore, the reduced performance of the KO Tmx P60 animals can be attributed to impaired autophagy during early adulthood (**Figure 18A**). Also, tamoxifen did not alter the exploration index of either genotype-related control animals

administered with tamoxifen or of the distinct treatment groups (KO Tmx P30, Het Tmx P30, KO Tmx P60, Het Tmx P60) (**Figure 18C**). Therefore, the not statistically significant reduced performance of KO Tmx P60 animals reflects a deficit of social memory and is not a consequence of limited exploration attempts due to reduced motivation to explore. The relatively limited sample size could again account for significant differences among the performances of individual animals that shape the overall group performance, thus limiting the statistical validity of these results. Also, autophagy impairment may exert unknown roles in the development of other limbic structures implicated in the processes of social cognition that do not relate with pruning. Overall, we do not report any significant deficits in sociability and social memory following neuronal autophagy impairment in either adolescence or early adulthood.

Recency memory, that is the ability to remember the temporal order in which different objects were explored, was studied using the TOR task. Tamoxifen administration did not cause any significant effects on the discrimination index of the genotype-related control animals compared to their untreated littermates. Impaired autophagy, however, contributed to the reduced performance of KO Tmx P30 animals, which significantly differed from that of Het Tmx P30, KO Tmx P60, and Het Tmx P60 mice (**Figure 19A**). Since tamoxifen administration did not affect the exploration index of any animal group (**Figure 19B**), the reduced performance of KO Tmx P30 animals, caused by impaired autophagy during adolescence, is indicative of defective recency memory. The mPFC and the perirhinal cortex (PRH) are implicated in the process of recency memory (Barker et al. 2007). Therefore, autophagy impairment during the-critical for the PFC synaptic pruning-time period of adolescence could explain the counterbalanced performance of mice in a task that requires proper PFC function. Why heterozygotes treated with tamoxifen during adolescence perform well in the task may be an artifact of the relatively limited sample size. Our data reveal that neuronal autophagy impairment during adolescence accounts for a compromised PFC development that contributes to recency memory deficits.

Studies generating specific lesions have identified that spatial memory, that is the ability to recall an object's location, relies on the proper function of the PRH, the hippocampus, and to some extent, the mPFC (Barker et al. 2007). In rodents, pruning in the hippocampus initiates around P25 (Faulkner, Low, and Cheng 2007), therefore, autophagy ablation starting at P31 should not cause major developmental deficits in this structure. Tamoxifen administration did not lead to discrimination index inconsistencies between untreated animals and genotype-related control mice treated with tamoxifen. A trend towards reduced discrimination of the displaced and the stationary object was observed for KO Tmx P30, KO Tmx P60, and Het Tmx P60 animals, with the difference in the performance of Het Tmx P60 and Het Tmx P30 being statistically significant. This reduced performance is attributed to autophagy impairment during adolescence and, interestingly, during early adulthood (**Figure 20A**). Tamoxifen administration per se did not alter the exploration index in any group (**Figure 20B**), suggesting that the poor performance in the OTP task arises from spatial memory deficits and is not an artifact of limited exploration attempts due to reduced motivation to explore. Again, the relatively limited sample size could explain the ameliorated performance of Het Tmx P30 mice compared to other treatment groups (KO Tmx P30, KO Tmx P60, Het Tmx P60). Our work indicates that impaired neuronal autophagy during adolescence and early adulthood leads to spatial memory deficits.

The PRH mainly underlies the novelty-recognition in mice, with mPFC's contribution being little if any (Barker et al. 2007). Therefore, we postulated that a deteriorated PFC pruning profile due to autophagy impairment would not lead to recognition-memory deficits. To this end, we performed the NOR task in the animal groups of interest. Tamoxifen administration did not affect the discrimination index of genotype-relate control mice compared to their untreated littermates, therefore, the reduced performance of KO Tmx P30 mice results from impaired autophagy and is independent of tamoxifen's effects as a drug. Surprisingly, KO Tmx P30 mice differed significantly in their performance compared to heterozygotes and conditional knockout animals with impaired autophagy at early adulthood (**Figure 21A**). Also, tamoxifen neither altered the exploration index of genotype-related control mice compared

to their untreated littermates, nor did it cause any differences in the exploration index among the distinct treatment groups (**Figure 21C**). Consequently, the poor performance of KO Tmx P30 mice in the NOR task is indicative of novelty-recognition deficits and does not arise from limited exploration attempts due to reduced motivation to explore. A greater number of animals participating in the NOR task could elucidate whether the positive discrimination index of Het Tmx P30 animals is an artifact of the relatively limited sample size. This unexpected deficit in novelty-recognition could be attributed to unknown effects of the impairment of basal autophagy. A presumptive synaptic pruning process in the PRH during adolescence, something that precedes our knowledge, would also explain these results and comprises an interesting field for further investigation.

E.3 Remarks on additional effects of neuronal autophagy impairment

Except for the increased PFC spine density and the behavioral deficits, *Thy1-Cre^{ERT2};atg5$^{f/f}$* animals exhibited additional abnormalities. Of note are some observed motor deficits, like tremor and difficulty in moving their back legs. Similar observations were made in *Atg5flox/flox; nestin-Cre* mice, in which *Atg5* is ablated from both neurons and glial cells, thus resulting in a more severe autophagy impaired profile. In particular, a*tg5flox/flox; nestin-Cre* mice exerted growth retardation, progressive motor and behavioral deficits, and reflexes indicative of neurodegeneration (limb-clasping reflexes). Motor deficits included ataxic walking, tremor, as well as impaired balance, motor coordination, and grip strength. Neurodegeneration was also verified with immunohistochemistry (Hara et al. 2006). In our case, behavioral experiments like the rotarod, the footprint analysis, and the wire-hanging would promote categorization of the observed motor deficits, while Nissl staining in the cerebellum of *Thy1-Cre^{ERT2};atg5$^{f/f}$* mice could identify morphological abnormalities underlying such phenotypes.

E.4 Study limitations and future perspectives

Our data indicate a direct link between autophagy and synaptic pruning that underlies proper PFC development. Increased mature spine densities followed the neuronal autophagy impairment in adolescence, and interestingly, in early adulthood, something that is indicative of limited synapse elimination due to inhibited synaptic pruning. Neither sociability nor social memory was substantially affected by neuronal autophagy impairment in either age. However, autophagy impairment during adolescence resulted in impeded recency memory and spatial memory. Spatial memory also deteriorated when autophagy was impaired during early adulthood, something that, combined with our current, and also previous, Golgi-cox staining data, leads us to postulate the existence of a second wave of synapse elimination, taking place in the PFC during early adulthood, that is important for its proper function. Defects were also observed in novelty-recognition, an ability that does not extensively rely on PFC function.

Increasing the sample size of these experiments would allow us to obtain more reliable results. Our repertoire of behavioral experiments could also be enriched with experiments like the rotarod, the footprint analysis, and the wire-hanging, to test for motor abnormalities. Impairing autophagy during early adulthood and studying the prefrontal cortical development and function is one of our main priorities in the foreseeable future. Another means of investigating how pruning is affected in response to autophagy impairment could be the study of synaptic properties, by performing extracellular field recordings. We expect that reduced autophagy levels resulting in impeded pruning affect LTP. Before looking for additional markers of synaptic plasticity, like synaptophysin or PDS-95, one should verify that autophagy is indeed impaired. Using transgenic mice that allow for visualizing the Cre-LoxP

recombination with confocal microscopy, like the Gt(ROSA)26Sor$^{tm4(ACTB-tdTomato,-EGFP)Luo}$/J mouse (The Jackson Laboratory strain 007676), would be a direct means of achieving this goal. Western-blot analysis or immunohistochemistry for autophagy markers, like LC3, ULK-1 or p62, is also needed. Transmission electron microscopy could be used to study autophagy vesicles between the experimental mice and control groups. It should be denoted that the *Thy1-Cre^{ERT2};atg5$^{f/f}$* mice used in our study exhibit milder autophagy impairment compared to a*tg5flox/flox; nestin-Cre* mice, therefore, the remaining glial autophagy could, to some extent, reverse the non-severe social cognition deficits noticed in the Three-Chamber Social Interaction task. The morphology of other structures implicated in functions supported, even partially, by the PFC, should definitely be studied, like for instance that of the PRH or amygdala. Potentially observed abnormalities in the cellular morphology of these areas will lead to a more precise experimental design towards explaining the observed phenotypes. Although not globally ablated, compromised autophagy can lead to neurodegeneration (Menzies et al. 2017), hence, additional experiments, like TUNEL staining of the cerebellum to quantify cell death, or staining for ubiquitin-positive inclusion bodies indicative of aggregated proteins, are needed.

Adolescence marks a period of massive hormonal changes with implications in PFC development (Bryan Kolb et al. 2012). Few studies have focused on hormonal-related alterations of neocortical dendritic spine density, and they indicate that spine arbor differs as a function of sex and age (B. Kolb and Stewart 1991; Bryan Kolb, Gibb, and Gorny 2003). Concerning the PFC, neuroimaging studies have associated testosterone with reduced cortical thickness and volume of gray matter in the frontal lobes in post-adolescent males (Nguyen et al. 2013; Koolschijn, Peper, and Crone 2014). On the contrary, recent work indicates that pruning of layer V pyramidal neurons during adolescence does not depend on gonadal hormones, as manipulation of ovarian hormones had an impact only on morphological maturation and dynamics (Boivin et al. 2018). More research is required on both male and female gonadal hormones to unravel the mechanisms that regulate such processes. In our study, analysis of preliminary data did not show any differences between the sexes. Last but not least, the ERT2, which is a mutation of the human estrogen receptor ligand-binding domain fused to Cre recombinase, does not bind its natural ligand (17β-estradiol) at physiological concentrations but does bind to the synthetic estrogen receptor ligands 4-hydroxytamoxifen (OHT or tamoxifen). A possibility for unwanted effects of estrogen signaling pathway activation cannot be ruled out, this way adding another level of complexity to our system. Future experiments entailing a greater sample size should take into account all these considerations.

Appendices

Appendix A

ABBREVIATION	GENOTYPE	TREATMENT	# OF ANIMALS IN THE SOCIABILITY TASK	# OF ANIMALS IN THE TOR TASK	# OF ANIMALS IN THE OTP TASK	# OF ANIMALS IN THE NOR TASK
KO Tmx P30	thy1-Cre^{ERT2};atg5$^{f/f}$	Tmx at P31-P35	5	5	6	4
Het Tmx P30	thy1-Cre^{ERT2};atg5$^{+/f}$	Tmx at P31-P35	7	8	8	6
KO Tmx P60	thy1-Cre^{ERT2};atg5$^{f/f}$	Tmx at P61-P65	5	6	4	5
Het Tmx P60	thy1-Cre^{ERT2};atg5$^{+/f}$	Tmx at P61-P65	3 in phase II, 2 in phase III	3	3	3
No Tmx or untreated animals	All possible genotypes	Oil	9	7	8	8
Tmx control or genotype-related control animals	thy1-Cre$^{ERT2(-)}$;atg5$^{f/f}$ or thy1-Cre$^{ERT2(-)}$;atg5$^{+/+}$ or thy1-Cre$^{ERT2(-)}$;atg5$^{+/f}$ or thy1-Cre^{ERT2};atg5$^{+/+}$	Tmx at P31-P35 or P61-P651	9 in phase II, 10 in phase III	11	10	9

Appendix B

The following line graphs denote the performance of untreated animals compared to genotype-related control animals in each behavioral experiment. Each line graph represents the performance of individual animals belonging to each of these control groups. The vertical axes show the amount of time each animal spent exploring each object or animal that is mentioned in the horizontal axis. Blue lines represent males, while pink lines represent females.

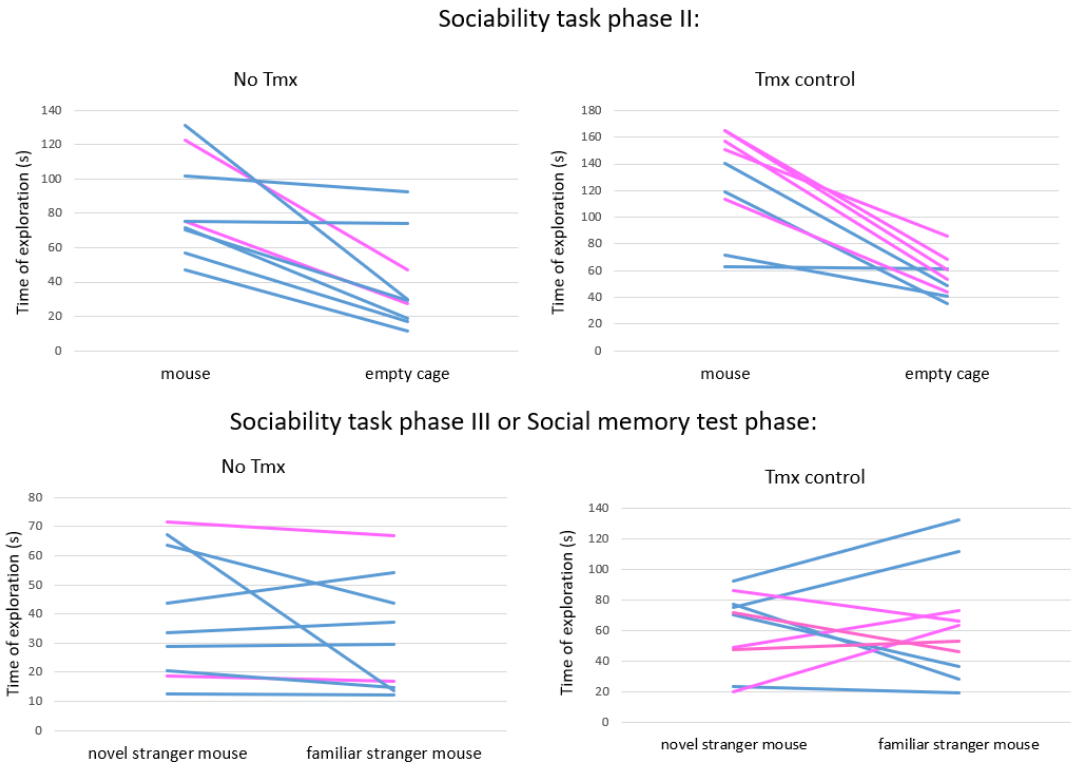

TOR task:

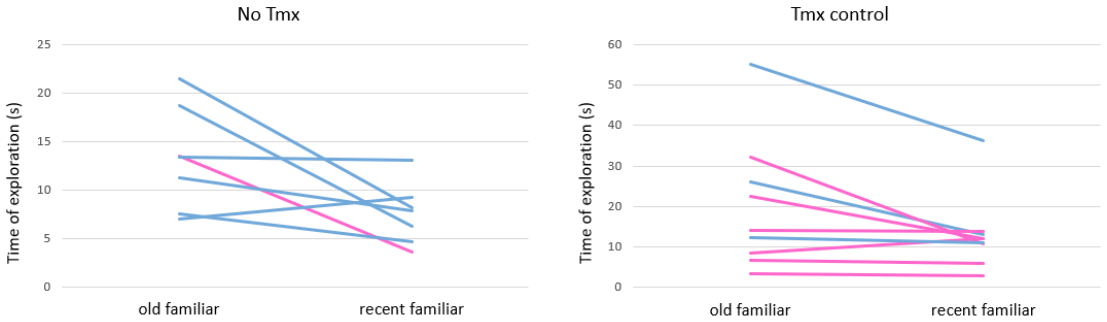

OTP task:

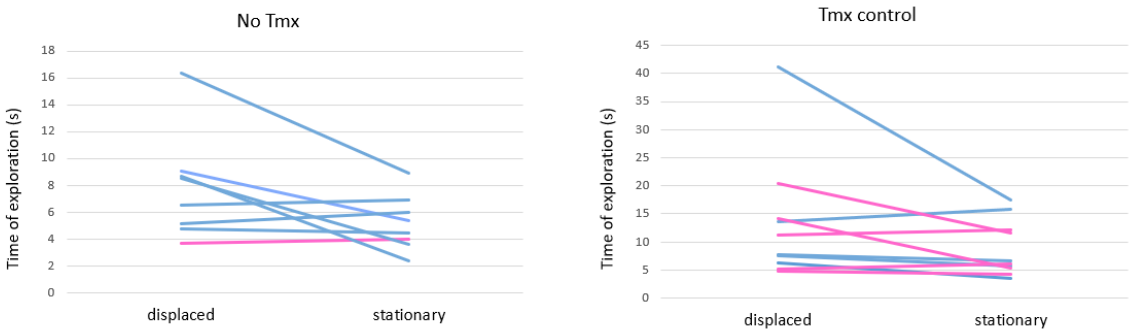

NOR task:

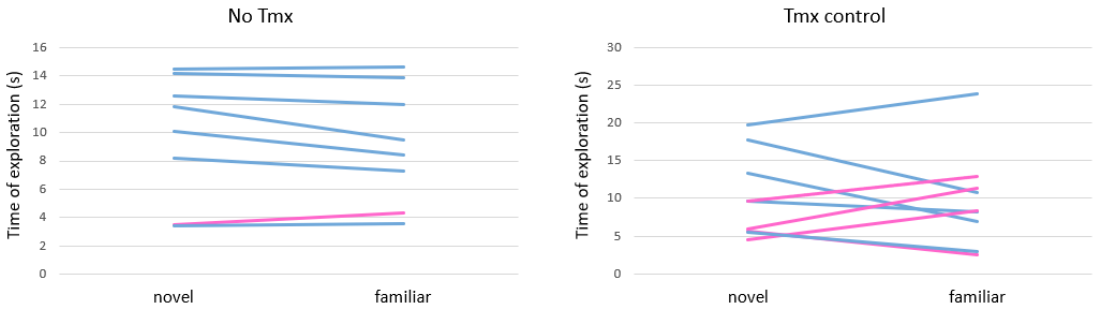

References

Afroz, Sonia, Julie Parato, Hui Shen, and Sheryl Sue Smith. 2016. “Synaptic Pruning in the Female Hippocampus Is Triggered at Puberty by Extrasynaptic GABAA Receptors on Dendritic Spines.” *eLife* 5 (May): e15106.

Amaral, D. G., and J. L. Price. 1984. “Amygdalo-Cortical Projections in the Monkey (Macaca Fascicularis).” *The Journal of Comparative Neurology* 230 (4): 465–96.

Arnsten, A. F., and P. S. Goldman-Rakic. 1998. “Noise Stress Impairs Prefrontal Cortical Cognitive Function in Monkeys: Evidence for a Hyperdopaminergic Mechanism.” *Archives of General Psychiatry* 55 (4): 362–68.

Awasaki, Takeshi, Yaling Huang, Michael B. O’Connor, and Tzumin Lee. 2011. “Glia Instruct Developmental Neuronal Remodeling through TGF-β Signaling.” *Nature Neuroscience* 14 (7): 821–23.

Bagri, Anil, Hwai-Jong Cheng, Avraham Yaron, Samuel J. Pleasure, and Marc Tessier-Lavigne. 2003. “Stereotyped Pruning of Long Hippocampal Axon Branches Triggered by Retraction Inducers of the Semaphorin Family.” *Cell* 113 (3): 285–99.

Barker, Gareth R. I., Flora Bird, Victoria Alexander, and E. Clea Warburton. 2007. “Recognition Memory for Objects, Place, and Temporal Order: A Disconnection Analysis of the Role of the Medial Prefrontal Cortex and Perirhinal Cortex.” *The Journal of Neuroscience: The Official Journal of the Society for Neuroscience* 27 (11): 2948–57.

Becker, Nadine, Corette J. Wierenga, Rosalina Fonseca, Tobias Bonhoeffer, and U. Valentin Nägerl. 2008. “LTD Induction Causes Morphological Changes of Presynaptic Boutons and Reduces Their Contacts with Spines.” *Neuron* 60 (4): 590–97.

Bellon, Anaïs, and Fanny Mann. 2018. “Keeping up with Advances in Axon Guidance.” *Current Opinion in Neurobiology* 53 (December): 183–91.

Berbel, P., and G. M. Innocenti. 1988. “The Development of the Corpus Callosum in Cats: A Light- and Electron-Microscopic Study.” *The Journal of Comparative Neurology* 276 (1): 132–56.

Bian, Wen-Jie, Wan-Ying Miao, Shun-Ji He, Zilong Qiu, and Xiang Yu. 2015. “Coordinated Spine Pruning and Maturation Mediated by Inter-Spine Competition for Cadherin/Catenin Complexes.” *Cell* 162 (4): 808–22.

Bicks, Lucy K., Hiroyuki Koike, Schahram Akbarian, and Hirofumi Morishita. 2015. “Prefrontal Cortex and Social Cognition in Mouse and Man.” *Frontiers in Psychology* 6 (November): 1805.

Binotti, Beyenech, Nathan J. Pavlos, Dietmar Riedel, Dirk Wenzel, Gerd Vorbrüggen, Amanda M. Schalk, Karin Kühnel, et al. 2015. “The GTPase Rab26 Links Synaptic Vesicles to the Autophagy Pathway.” *eLife* 4 (February): e05597.

Bishop, Derron L., Thomas Misgeld, Mark K. Walsh, Wen-Biao Gan, and Jeff W. Lichtman. 2004. “Axon Branch Removal at Developing Synapses by Axosome Shedding.” *Neuron* 44 (4): 651–61.

Boivin, Josiah R., David J. Piekarski, A. Wren Thomas, and Linda Wilbrecht. 2018. “Adolescent Pruning and Stabilization of Dendritic Spines on Cortical Layer 5 Pyramidal Neurons Do Not Depend on Gonadal Hormones.” *Developmental Cognitive Neuroscience* 30 (April): 100–107.

Boulanger, Ana, Christelle Clouet-Redt, Morgane Farge, Adrien Flandre, Thomas Guignard, Céline Fernando, François Juge, and Jean-Maurice Dura. 2010. “Ftz-f1 and Hr39 Opposing Roles on EcR Expression during Drosophila Mushroom Body Neuron Remodeling.” *Nature Neuroscience* 14 (1): 37–44.

Breunig, Joshua J., Tarik F. Haydar, and Pasko Rakic. 2011. “Neural Stem Cells: Historical Perspective and Future Prospects.” *Neuron* 70 (4): 614–25.

Brodal, Per. 2004. *The Central Nervous System: Structure and Function*. Oxford University Press.

Burkhalter, A., and K. L. Bernardo. 1989. “Organization of Corticocortical Connections in Human Visual Cortex.” *Proceedings of the National Academy of Sciences of the United States of America* 86 (3): 1071–75.
Buyanova, Irina S., and Marie Arsalidou. 2021. “Cerebral White Matter Myelination and Relations to Age, Gender, and Cognition: A Selective Review.” *Frontiers in Human Neuroscience*. https://doi.org/10.3389/fnhum.2021.662031.
Carlén, Marie. 2017. “What Constitutes the Prefrontal Cortex?” *Science* 358 (6362): 478–82.
Chen, Mark, Janice A. Maloney, Dara Y. Kallop, Jasvinder K. Atwal, Stephen J. Tam, Kristin Baer, Holger Kissel, et al. 2012. “Spatially Coordinated Kinase Signaling Regulates Local Axon Degeneration.” *The Journal of Neuroscience: The Official Journal of the Society for Neuroscience* 32 (39): 13439–53.
Chidambaram, Saravana Babu, A. G. Rathipriya, Srinivasa Rao Bolla, Abid Bhat, Bipul Ray, Arehally Marappa Mahalakshmi, Thamilarasan Manivasagam, et al. 2019. “Dendritic Spines: Revisiting the Physiological Role.” *Progress in Neuro-Psychopharmacology & Biological Psychiatry* 92 (June): 161–93.
Choi, B. H. 1981. “Radial Glia of Developing Human Fetal Spinal Cord: Golgi, Immunohistochemical and Electron Microscopic Study.” *Brain Research* 227 (2): 249–67.
Choi, B. H., and L. W. Lapham. 1978. “Radial Glia in the Human Fetal Cerebrum: A Combined Golgi, Immunofluorescent and Electron Microscopic Study.” *Brain Research* 148 (2): 295–311.
Chou, Shen-Ju, Zoila Babot, Axel Leingärtner, Michele Studer, Yasushi Nakagawa, and Dennis D. M. O’Leary. 2013. “Geniculocortical Input Drives Genetic Distinctions between Primary and Higher-Order Visual Areas.” *Science* 340 (6137): 1239–42.
Chung, Won-Suk, Laura E. Clarke, Gordon X. Wang, Benjamin K. Stafford, Alexander Sher, Chandrani Chakraborty, Julia Joung, et al. 2013. “Astrocytes Mediate Synapse Elimination through MEGF10 and MERTK Pathways.” *Nature* 504 (7480): 394–400.
Clarke, Laura E., and Ben A. Barres. 2013. “Emerging Roles of Astrocytes in Neural Circuit Development.” *Nature Reviews. Neuroscience* 14 (5): 311–21.
Cusack, Corey L., Vijay Swahari, W. Hampton Henley, J. Michael Ramsey, and Mohanish Deshmukh. 2013. “Distinct Pathways Mediate Axon Degeneration during Apoptosis and Axon-Specific Pruning.” *Nature Communications* 4: 1876.
Delevich, Kristen, A. Wren Thomas, and Linda Wilbrecht. 2018. “Adolescence and ‘Late Blooming’ Synapses of the Prefrontal Cortex.” *Cold Spring Harbor Symposia on Quantitative Biology* 83: 37–43.
Dupre, Christophe, and Rafael Yuste. 2017. “Non-Overlapping Neural Networks in Hydra Vulgaris.” *Current Biology: CB* 27 (8): 1085–97.
Faulkner, Regina L., Lawrence K. Low, and Hwai-Jong Cheng. 2007. “Axon Pruning in the Developing Vertebrate Hippocampus.” *Developmental Neuroscience* 29 (1-2): 6–13.
Feil, Susanne, Nadejda Valtcheva, and Robert Feil. 2009. “Inducible Cre Mice.” *Methods in Molecular Biology* 530: 343–63.
Feng, Yuchen, Ding He, Zhiyuan Yao, and Daniel J. Klionsky. 2014. “The Machinery of Macroautophagy.” *Cell Research* 24 (1): 24–41.
Fields, R. Douglas. 2015. “A New Mechanism of Nervous System Plasticity: Activity-Dependent Myelination.” *Nature Reviews. Neuroscience* 16 (12): 756–67.
Füllgrabe, Jens, Daniel J. Klionsky, and Bertrand Joseph. 2014. “The Return of the Nucleus: Transcriptional and Epigenetic Control of Autophagy.” *Nature Reviews. Molecular Cell Biology* 15 (1): 65–74.
Fuster, Joaquín M. 2002. “Frontal Lobe and Cognitive Development.” *Journal of Neurocytology* 31 (3-5): 373–85.

Gerdts, Josiah, Yo Sasaki, Bhupinder Vohra, Jayne Marasa, and Jeffrey Milbrandt. 2011. “Image-Based Screening Identifies Novel Roles for IkappaB Kinase and Glycogen Synthase Kinase 3 in Axonal Degeneration.” *The Journal of Biological Chemistry* 286 (32): 28011–18.
Ghosh, Arundhati Sengupta, Bei Wang, Christine D. Pozniak, Mark Chen, Ryan J. Watts, and Joseph W. Lewcock. 2011. “DLK Induces Developmental Neuronal Degeneration via Selective Regulation of Proapoptotic JNK Activity.” *The Journal of Cell Biology* 194 (5): 751–64.
Gladding, Clare M., Stephen M. Fitzjohn, and Elek Molnár. 2009. “Metabotropic Glutamate Receptor-Mediated Long-Term Depression: Molecular Mechanisms.” *Pharmacological Reviews* 61 (4): 395–412.
Glick, Danielle, Sandra Barth, and Kay F. Macleod. 2010. “Autophagy: Cellular and Molecular Mechanisms.” *The Journal of Pathology* 221 (1): 3–12.
Hara, Taichi, Kenji Nakamura, Makoto Matsui, Akitsugu Yamamoto, Yohko Nakahara, Rika Suzuki-Migishima, Minesuke Yokoyama, et al. 2006. “Suppression of Basal Autophagy in Neural Cells Causes Neurodegenerative Disease in Mice.” *Nature* 441 (7095): 885–89.
He, Fei, and Yi E. Sun. 2007. “Glial Cells More than Support Cells?” *The International Journal of Biochemistry & Cell Biology*. https://doi.org/10.1016/j.biocel.2006.10.022.
Hoerder-Suabedissen, Anna, and Zoltán Molnár. 2015. “Development, Evolution and Pathology of Neocortical Subplate Neurons.” *Nature Reviews. Neuroscience* 16 (3): 133–46.
Holtmaat, Anthony, and Karel Svoboda. 2009. “Experience-Dependent Structural Synaptic Plasticity in the Mammalian Brain.” *Nature Reviews. Neuroscience* 10 (9): 647–58.
Horton, Jonathan C., and Daniel L. Adams. 2005. “The Cortical Column: A Structure without a Function.” *Philosophical Transactions of the Royal Society of London. Series B, Biological Sciences* 360 (1456): 837–62.
Hotulainen, Pirta, and Casper C. Hoogenraad. 2010. “Actin in Dendritic Spines: Connecting Dynamics to Function.” *The Journal of Cell Biology* 189 (4): 619–29.
Howard, Brian M., Zhicheng Mo, Radmila Filipovic, Anna R. Moore, Srdjan D. Antic, and Nada Zecevic. 2008. “Radial Glia Cells in the Developing Human Brain.” *The Neuroscientist: A Review Journal Bringing Neurobiology, Neurology and Psychiatry* 14 (5): 459–73.
Huang, Jingxiang, Christian C. Dibble, Mika Matsuzaki, and Brendan D. Manning. 2008. “The TSC1-TSC2 Complex Is Required for Proper Activation of mTOR Complex 2.” *Molecular and Cellular Biology* 28 (12): 4104–15.
Huang, Yan-You, Eleanor Simpson, Christoph Kellendonk, and Eric R. Kandel. 2004. “Genetic Evidence for the Bidirectional Modulation of Synaptic Plasticity in the Prefrontal Cortex by D1 Receptors.” *Proceedings of the National Academy of Sciences of the United States of America* 101 (9): 3236–41.
Huttenlocher, P. R. 1979. “Synaptic Density in Human Frontal Cortex - Developmental Changes and Effects of Aging.” *Brain Research* 163 (2): 195–205.
Hwang, Jee-Yeon, Jingqi Yan, and Ruth Suzanne Zukin. 2019. “Autophagy and Synaptic Plasticity: Epigenetic Regulation.” *Current Opinion in Neurobiology* 59 (December): 207–12.
Jakovcevski, Igor, Radmila Filipovic, Zhicheng Mo, Sonja Rakic, and Nada Zecevic. 2009. “Oligodendrocyte Development and the Onset of Myelination in the Human Fetal Brain.” *Frontiers in Neuroanatomy* 3 (June): 5.
Jay, Thérèse M., Cyril Rocher, Maïte Hotte, Laurent Naudon, Hirac Gurden, and Michael Spedding. 2004. “Plasticity at Hippocampal to Prefrontal Cortex Synapses Is Impaired by Loss of Dopamine and Stress: Importance for Psychiatric Diseases.” *Neurotoxicity Research* 6 (3): 233–44.
Jung, Chang Hwa, Chang Bong Jun, Seung-Hyun Ro, Young-Mi Kim, Neil Michael Otto, Jing Cao, Mondira Kundu, and Do-Hyung Kim. 2009. “ULK-Atg13-FIP200 Complexes Mediate mTOR Signaling to the Autophagy Machinery.” *Molecular Biology of the Cell* 20 (7): 1992–2003.

Kaczmarczyk, Lech, and Walker S. Jackson. 2015. “Astonishing Advances in Mouse Genetic Tools for Biomedical Research.” *Swiss Medical Weekly* 145 (October): w14186.
Kallergi, Emmanouela, Akrivi-Dimitra Daskalaki, Evangelia Ioannou, Angeliki Kolaxi, Maria Plataki, Per Haberkant, Frank Stein, et al. 2020. “Long-Term Synaptic Depression Triggers Local Biogenesis of Autophagic Vesicles in Dendrites and Requires Autophagic Degradation.” *bioRxiv*. https://doi.org/10.1101/2020.03.12.983965.
Kandel, Eric R. 2013. *Principles of Neural Science*.
Katz, L. C., and C. J. Shatz. 1996. “Synaptic Activity and the Construction of Cortical Circuits.” *Science* 274 (5290): 1133–38.
Kim, H-J, M-H Cho, W. H. Shim, J. K. Kim, E-Y Jeon, D-H Kim, and S-Y Yoon. 2017. “Deficient Autophagy in Microglia Impairs Synaptic Pruning and Causes Social Behavioral Defects.” *Molecular Psychiatry* 22 (11): 1576–84.
Kirilly, Daniel, Ying Gu, Yafen Huang, Zhuhao Wu, Arash Bashirullah, Boon Chuan Low, Alex L. Kolodkin, Hongyan Wang, and Fengwei Yu. 2009. “A Genetic Pathway Composed of Sox14 and Mical Governs Severing of Dendrites during Pruning.” *Nature Neuroscience* 12 (12): 1497–1505.
Klionsky, Daniel J., James M. Cregg, William A. Dunn Jr, Scott D. Emr, Yasuyoshi Sakai, Ignacio V. Sandoval, Andrei Sibirny, et al. 2003. “A Unified Nomenclature for Yeast Autophagy-Related Genes.” *Developmental Cell* 5 (4): 539–45.
Klune, Cassandra B., Benita Jin, and Laura A. DeNardo. 2021. “Linking mPFC Circuit Maturation to the Developmental Regulation of Emotional Memory and Cognitive Flexibility.” *eLife* 10 (May). https://doi.org/10.7554/eLife.64567.
Kolb, Bryan, Robbin Gibb, and Grazyna Gorny. 2003. “Experience-Dependent Changes in Dendritic Arbor and Spine Density in Neocortex Vary Qualitatively with Age and Sex.” *Neurobiology of Learning and Memory* 79 (1): 1–10.
Kolb, Bryan, Richelle Mychasiuk, Arif Muhammad, Yilin Li, Douglas O. Frost, and Robbin Gibb. 2012. “Experience and the Developing Prefrontal Cortex.” *Proceedings of the National Academy of Sciences of the United States of America* 109 (Supplement 2): 17186–93.
Kolb, B., and J. Stewart. 1991. “Sex-Related Differences in Dendritic Branching of Cells in the Prefrontal Cortex of Rats.” *Journal of Neuroendocrinology* 3 (1): 95–99.
Koolschijn, P. Cédric M. P., Jiska S. Peper, and Eveline A. Crone. 2014. “The Influence of Sex Steroids on Structural Brain Maturation in Adolescence.” *PloS One* 9 (1): e83929.
Kostovic, I., and P. Rakic. 1990. “Developmental History of the Transient Subplate Zone in the Visual and Somatosensory Cortex of the Macaque Monkey and Human Brain.” *The Journal of Comparative Neurology* 297 (3): 441–70.
Kroemer, Guido, Guillermo Mariño, and Beth Levine. 2010. “Autophagy and the Integrated Stress Response.” *Molecular Cell* 40 (2): 280–93.
Kuhn, Sarah, Laura Gritti, Daniel Crooks, and Yvonne Dombrowski. 2019. “Oligodendrocytes in Development, Myelin Generation and Beyond.” *Cells* 8 (11). https://doi.org/10.3390/cells8111424.
Laplante, Mathieu, and David M. Sabatini. 2012. “mTOR Signaling in Growth Control and Disease.” *Cell* 149 (2): 274–93.
Laubach, Mark, Linda M. Amarante, Kyra Swanson, and Samantha R. White. 2018. “What, If Anything, Is Rodent Prefrontal Cortex?” *eNeuro* 5 (5). https://doi.org/10.1523/ENEURO.0315-18.2018.
Lieberman, Ori J., Avery F. McGuirt, Guomei Tang, and David Sulzer. 2019. “Roles for Neuronal and Glial Autophagy in Synaptic Pruning during Development.” *Neurobiology of Disease* 122 (February): 49–63.

Loncle, Nicolas, and Darren W. Williams. 2012. “An Interaction Screen Identifies Headcase as a Regulator of Large-Scale Pruning.” *The Journal of Neuroscience: The Official Journal of the Society for Neuroscience* 32 (48): 17086–96.
Low, Lawrence K., Xiao-Bo Liu, Regina L. Faulkner, Jeffrey Coble, and Hwai-Jong Cheng. 2008. “Plexin Signaling Selectively Regulates the Stereotyped Pruning of Corticospinal Axons from Visual Cortex.” *Proceedings of the National Academy of Sciences of the United States of America* 105 (23): 8136–41.
Luduena, R. F., W. H. Anderson, V. Prasad, M. A. Jordan, K. C. Ferrigni, M. C. Roach, P. M. Horowitz, D. B. Murphy, and A. Fellous. 1986. “Interactions of Vinblastine and Maytansine with Tubulin.” *Annals of the New York Academy of Sciences* 466: 718–32.
Maor-Nof, Maya, Noriko Homma, Calanit Raanan, Aviv Nof, Nobutaka Hirokawa, and Avraham Yaron. 2013. “Axonal Pruning Is Actively Regulated by the Microtubule-Destabilizing Protein Kinesin Superfamily Protein 2A.” *Cell Reports* 3 (4): 971–77.
Maor-Nof, Maya, and Avraham Yaron. 2013. “Neurite Pruning and Neuronal Cell Death: Spatial Regulation of Shared Destruction Programs.” *Current Opinion in Neurobiology* 23 (6): 990–96.
Marín, Oscar. 2016. “Developmental Timing and Critical Windows for the Treatment of Psychiatric Disorders.” *Nature Medicine* 22 (11): 1229–38.
Menzies, Fiona M., Angeleen Fleming, Andrea Caricasole, Carla F. Bento, Stephen P. Andrews, Avraham Ashkenazi, Jens Füllgrabe, et al. 2017. “Autophagy and Neurodegeneration: Pathogenic Mechanisms and Therapeutic Opportunities.” *Neuron* 93 (5): 1015–34.
Merenlender-Wagner, A., A. Malishkevich, Z. Shemer, M. Udawela, A. Gibbons, E. Scarr, B. Dean, J. Levine, G. Agam, and I. Gozes. 2015. “Autophagy Has a Key Role in the Pathophysiology of Schizophrenia.” *Molecular Psychiatry* 20 (1): 126–32.
Mizushima, Noboru, and Masaaki Komatsu. 2011. “Autophagy: Renovation of Cells and Tissues.” *Cell* 147 (4): 728–41.
Mountcastle, V. 1997. “The Columnar Organization of the Neocortex.” *Brain*. https://doi.org/10.1093/brain/120.4.701.
Mrzljak, L., H. B. Uylings, I. Kostovic, and C. G. Van Eden. 1988. “Prenatal Development of Neurons in the Human Prefrontal Cortex: I. A Qualitative Golgi Study.” *The Journal of Comparative Neurology* 271 (3): 355–86.
Nakatogawa, Hitoshi, Kuninori Suzuki, Yoshiaki Kamada, and Yoshinori Ohsumi. 2009. “Dynamics and Diversity in Autophagy Mechanisms: Lessons from Yeast.” *Nature Reviews. Molecular Cell Biology* 10 (7): 458–67.
Nguyen, Tuong-Vi, James McCracken, Simon Ducharme, Kelly N. Botteron, Megan Mahabir, Wendy Johnson, Mimi Israel, Alan C. Evans, Sherif Karama, and Brain Development Cooperative Group. 2013. “Testosterone-Related Cortical Maturation across Childhood and Adolescence.” *Cerebral Cortex* 23 (6): 1424–32.
Nikolaev, Anatoly, Todd McLaughlin, Dennis D. M. O’Leary, and Marc Tessier-Lavigne. 2009. “APP Binds DR6 to Trigger Axon Pruning and Neuron Death via Distinct Caspases.” *Nature* 457 (7232): 981–89.
Nikoletopoulou, Vassiliki, Kyriaki Sidiropoulou, Emmanouela Kallergi, Yannis Dalezios, and Nektarios Tavernarakis. 2017. “Modulation of Autophagy by BDNF Underlies Synaptic Plasticity.” *Cell Metabolism* 26 (1): 230–42.e5.
Okado, N., S. Kakimi, and T. Kojima. 1979. “Synaptogenesis in the Cervical Cord of the Human Embryo: Sequence of Synapse Formation in a Spinal Reflex Pathway.” *The Journal of Comparative Neurology* 184 (3): 491–518.

Okerlund, Nathan D., Katharina Schneider, Sergio Leal-Ortiz, Carolina Montenegro-Venegas, Sally A. Kim, Loren C. Garner, Clarissa L. Waites, Eckart D. Gundelfinger, Richard J. Reimer, and Craig C. Garner. 2017. "Bassoon Controls Presynaptic Autophagy through Atg5." *Neuron* 93 (4): 897–913.e7.
O'Leary, D. D., and S. E. Koester. 1993. "Development of Projection Neuron Types, Axon Pathways, and Patterned Connections of the Mammalian Cortex." *Neuron* 10 (6): 991–1006.
Palomero-Gallagher, Nicola, and Karl Zilles. 2019. "Cortical Layers: Cyto-, Myelo-, Receptor- and Synaptic Architecture in Human Cortical Areas." *NeuroImage* 197 (August): 716–41.
Pchitskaya, Ekaterina, and Ilya Bezprozvanny. 2020. "Dendritic Spines Shape Analysis-Classification or Clusterization? Perspective." *Frontiers in Synaptic Neuroscience* 12 (September): 31.
Penagarikano, Olga, Jennifer G. Mulle, and Stephen T. Warren. 2007. "The Pathophysiology of Fragile X Syndrome." *Annual Review of Genomics and Human Genetics* 8: 109–29.
Petanjek, Zdravko, Miloš Judaš, Goran Šimić, Mladen Roko Rašin, Harry B. M. Uylings, Pasko Rakic, and Ivica Kostović. 2011. "Extraordinary Neoteny of Synaptic Spines in the Human Prefrontal Cortex." *Proceedings of the National Academy of Sciences of the United States of America* 108 (32): 13281–86.
Phillips, Mary, and Lucas Pozzo-Miller. 2015. "Dendritic Spine Dysgenesis in Autism Related Disorders." *Neuroscience Letters* 601 (August): 30–40.
Piochon, Claire, Masanobu Kano, and Christian Hansel. 2016. "LTD-like Molecular Pathways in Developmental Synaptic Pruning." *Nature Neuroscience* 19 (10): 1299–1310.
Portera-Cailliau, Carlos, David T. Pan, and Rafael Yuste. 2003. "Activity-Regulated Dynamic Behavior of Early Dendritic Protrusions: Evidence for Different Types of Dendritic Filopodia." *The Journal of Neuroscience: The Official Journal of the Society for Neuroscience* 23 (18): 7129–42.
Portera Cailliau, C., and R. Yuste. 2001. "[On the function of dendritic filopodia]." *Revista de neurologia* 33 (12): 1158–66.
Poultney, Christopher S., Arthur P. Goldberg, Elodie Drapeau, Yan Kou, Hala Harony-Nicolas, Yuji Kajiwara, Silvia De Rubeis, et al. 2013. "Identification of Small Exonic CNV from Whole-Exome Sequence Data and Application to Autism Spectrum Disorder." *American Journal of Human Genetics* 93 (4): 607–19.
Ramaswamy, Srikanth, and Henry Markram. 2015. "Anatomy and Physiology of the Thick-Tufted Layer 5 Pyramidal Neuron." *Frontiers in Cellular Neuroscience* 9 (June): 233.
Riccomagno, Martin M., Andrés Hurtado, Hongbin Wang, Joshua G. J. Macopson, Erin M. Griner, Andrea Betz, Nils Brose, Marcelo G. Kazanietz, and Alex L. Kolodkin. 2012. "The RacGAP β2-Chimaerin Selectively Mediates Axonal Pruning in the Hippocampus." *Cell* 149 (7): 1594–1606.
Riccomagno, Martin M., and Alex L. Kolodkin. 2015. "Sculpting Neural Circuits by Axon and Dendrite Pruning." *Annual Review of Cell and Developmental Biology* 31 (October): 779–805.
Rowland, Aaron M., Janet E. Richmond, Jason G. Olsen, David H. Hall, and Bruce A. Bamber. 2006. "Presynaptic Terminals Independently Regulate Synaptic Clustering and Autophagy of GABAA Receptors in Caenorhabditis Elegans." *The Journal of Neuroscience: The Official Journal of the Society for Neuroscience* 26 (6): 1711–20.
Rubio-Garrido, Pablo, Flor Pérez-de-Manzo, César Porrero, Maria J. Galazo, and Francisco Clascá. 2009. "Thalamic Input to Distal Apical Dendrites in Neocortical Layer 1 Is Massive and Highly Convergent." *Cerebral Cortex* 19 (10): 2380–95.
Russell, Ryan C., Ye Tian, Haixin Yuan, Hyun Woo Park, Yu-Yun Chang, Joungmok Kim, Haerin Kim, Thomas P. Neufeld, Andrew Dillin, and Kun-Liang Guan. 2013. "ULK1 Induces Autophagy by Phosphorylating Beclin-1 and Activating VPS34 Lipid Kinase." *Nature Cell Biology* 15 (7): 741–50.
Schafer, Dorothy P., Emily K. Lehrman, Amanda G. Kautzman, Ryuta Koyama, Alan R. Mardinly, Ryo Yamasaki, Richard M. Ransohoff, Michael E. Greenberg, Ben A. Barres, and Beth Stevens. 2012. "Microglia Sculpt Postnatal Neural Circuits in an Activity and Complement-Dependent Manner." *Neuron* 74 (4): 691–705.

Schmithorst, Vincent J., Marko Wilke, Bernard J. Dardzinski, and Scott K. Holland. 2002. “Correlation of White Matter Diffusivity and Anisotropy with Age during Childhood and Adolescence: A Cross-Sectional Diffusion-Tensor MR Imaging Study.” *Radiology* 222 (1): 212–18.
Schuck, Sebastian. 2020. “Microautophagy - Distinct Molecular Mechanisms Handle Cargoes of Many Sizes.” *Journal of Cell Science* 133 (17). https://doi.org/10.1242/jcs.246322.
Schuldiner, Oren, Daniela Berdnik, Jonathan Ma Levy, Joy S. Wu, David Luginbuhl, Allison Camille Gontang, and Liqun Luo. 2008. “piggyBac-Based Mosaic Screen Identifies a Postmitotic Function for Cohesin in Regulating Developmental Axon Pruning.” *Developmental Cell* 14 (2): 227–38.
Schuldiner, Oren, and Avraham Yaron. 2015. “Mechanisms of Developmental Neurite Pruning.” *Cellular and Molecular Life Sciences: CMLS* 72 (1): 101–19.
Sdrulla, Andrei D., and David J. Linden. 2007. “Double Dissociation between Long-Term Depression and Dendritic Spine Morphology in Cerebellar Purkinje Cells.” *Nature Neuroscience* 10 (5): 546–48.
Selemon, L. D., and N. Zecevic. 2015. “Schizophrenia: A Tale of Two Critical Periods for Prefrontal Cortical Development.” *Translational Psychiatry* 5 (8): e623–e623.
Sexton, Claire E., Kristine B. Walhovd, Andreas B. Storsve, Christian K. Tamnes, Lars T. Westlye, Heidi Johansen-Berg, and Anders M. Fjell. 2014. “Accelerated Changes in White Matter Microstructure during Aging: A Longitudinal Diffusion Tensor Imaging Study.” *The Journal of Neuroscience: The Official Journal of the Society for Neuroscience* 34 (46): 15425–36.
Shapiro, Lauren P., Ryan G. Parsons, Anthony J. Koleske, and Shannon L. Gourley. 2017. “Differential Expression of Cytoskeletal Regulatory Factors in the Adolescent Prefrontal Cortex: Implications for Cortical Development.” *Journal of Neuroscience Research* 95 (5): 1123–43.
Shehata, Mohammad, Hiroyuki Matsumura, Reiko Okubo-Suzuki, Noriaki Ohkawa, and Kaoru Inokuchi. 2012. “Neuronal Stimulation Induces Autophagy in Hippocampal Neurons That Is Involved in AMPA Receptor Degradation after Chemical Long-Term Depression.” *The Journal of Neuroscience: The Official Journal of the Society for Neuroscience* 32 (30): 10413–22.
Shibata, Mikihito, Forrest O. Gulden, and Nenad Sestan. 2015. “From Trans to Cis: Transcriptional Regulatory Networks in Neocortical Development.” *Trends in Genetics: TIG* 31 (2): 77–87.
Silbereis, John C., Sirisha Pochareddy, Ying Zhu, Mingfeng Li, and Nenad Sestan. 2016. “The Cellular and Molecular Landscapes of the Developing Human Central Nervous System.” *Neuron* 89 (2): 248–68.
Simon Wiegert, J., and Thomas G. Oertner. 2013. “Long-Term Depression Triggers the Selective Elimination of Weakly Integrated Synapses.” *Proceedings of the National Academy of Sciences of the United States of America* 110 (47): E4510–19.
Singh, Karun K., Katya J. Park, Elizabeth J. Hong, Bianca M. Kramer, Michael E. Greenberg, David R. Kaplan, and Freda D. Miller. 2008. “Developmental Axon Pruning Mediated by BDNF-p75NTR-Dependent Axon Degeneration.” *Nature Neuroscience* 11 (6): 649–58.
Slater, David A., Lester Melie-Garcia, Martin Preisig, Ferath Kherif, Antoine Lutti, and Bogdan Draganski. 2019. “Evolution of White Matter Tract Microstructure across the Life Span.” *Human Brain Mapping* 40 (7): 2252–68.
Sragovich, Shlomo, Avia Merenlender-Wagner, and Illana Gozes. 2017. “ADNP Plays a Key Role in Autophagy: From Autism to Schizophrenia and Alzheimer’s Disease.” *BioEssays: News and Reviews in Molecular, Cellular and Developmental Biology* 39 (11). https://doi.org/10.1002/bies.201700054.
Staiger, Jochen F., Iris Flagmeyer, Dirk Schubert, Karl Zilles, Rolf Kötter, and Heiko J. Luhmann. 2004. “Functional Diversity of Layer IV Spiny Neurons in Rat Somatosensory Cortex: Quantitative Morphology of Electrophysiologically Characterized and Biocytin Labeled Cells.” *Cerebral Cortex* 14 (6): 690–701.
Striedter, Georg F. 2006. “Précis of Principles of Brain Evolution.” *The Behavioral and Brain Sciences* 29 (1): 1–12; discussion 12–36.

Tang, Guomei, Kathryn Gudsnuk, Sheng-Han Kuo, Marisa L. Cotrina, Gorazd Rosoklija, Alexander Sosunov, Mark S. Sonders, et al. 2014. “Loss of mTOR-Dependent Macroautophagy Causes Autistic-like Synaptic Pruning Deficits.” *Neuron* 83 (5): 1131–43.
Tanida, Isei, Takashi Ueno, and Eiki Kominami. 2008. “LC3 and Autophagy.” *Methods in Molecular Biology* 445: 77–88.
Technau, G., and M. Heisenberg. 1982. “Neural Reorganization during Metamorphosis of the Corpora Pedunculata in Drosophila Melanogaster.” *Nature* 295 (5848): 405–7.
Thomson, Alex M. 2010. “Neocortical Layer 6, a Review.” *Frontiers in Neuroanatomy* 4 (March): 13.
Tooze, Sharon A., and Tamotsu Yoshimori. 2010. “The Origin of the Autophagosomal Membrane.” *Nature Cell Biology* 12 (9): 831–35.
Uesaka, Naofumi, Motokazu Uchigashima, Takayasu Mikuni, Takanobu Nakazawa, Harumi Nakao, Hirokazu Hirai, Atsu Aiba, Masahiko Watanabe, and Masanobu Kano. 2014. “Retrograde Semaphorin Signaling Regulates Synapse Elimination in the Developing Mouse Brain.” *Science* 344 (6187): 1020–23.
Vanhauwaert, Roeland, Sabine Kuenen, Roy Masius, Adekunle Bademosi, Julia Manetsberger, Nils Schoovaerts, Laura Bounti, et al. 2017. “The SAC1 Domain in Synaptojanin Is Required for Autophagosome Maturation at Presynaptic Terminals.” *The EMBO Journal* 36 (10): 1392–1411.
Vogt, B. A., and D. N. Pandya. 1978. “Cortico-Cortical Connections of Somatic Sensory Cortex (areas 3, 1 and 2) in the Rhesus Monkey.” *The Journal of Comparative Neurology* 177 (2): 179–91.
Wang, Xiao-Bin, Yunlei Yang, and Qiang Zhou. 2007. “Independent Expression of Synaptic and Morphological Plasticity Associated with Long-Term Depression.” *The Journal of Neuroscience: The Official Journal of the Society for Neuroscience* 27 (45): 12419–29.
Wen, Quan, Armen Stepanyants, Guy N. Elston, Alexander Y. Grosberg, and Dmitri B. Chklovskii. 2009. “Maximization of the Connectivity Repertoire as a Statistical Principle Governing the Shapes of Dendritic Arbors.” *Proceedings of the National Academy of Sciences of the United States of America* 106 (30): 12536–41.
Westlye, Lars T., Kristine B. Walhovd, Anders M. Dale, Atle Bjørnerud, Paulina Due-Tønnessen, Andreas Engvig, Håkon Grydeland, Christian K. Tamnes, Ylva Ostby, and Anders M. Fjell. 2010. “Life-Span Changes of the Human Brain White Matter: Diffusion Tensor Imaging (DTI) and Volumetry.” *Cerebral Cortex* 20 (9): 2055–68.
Williams, Darren W., and James W. Truman. 2005. “Cellular Mechanisms of Dendrite Pruning in Drosophila: Insights from in Vivo Time-Lapse of Remodeling Dendritic Arborizing Sensory Neurons.” *Development* 132 (16): 3631–42.
Xu, Nan-Jie, and Mark Henkemeyer. 2009. “Ephrin-B3 Reverse Signaling through Grb4 and Cytoskeletal Regulators Mediates Axon Pruning.” *Nature Neuroscience* 12 (3): 268–76.
Yang, Jing, Robby M. Weimer, Dara Kallop, Olav Olsen, Zhuhao Wu, Nicolas Renier, Kunihiro Uryu, and Marc Tessier-Lavigne. 2013. “Regulation of Axon Degeneration after Injury and in Development by the Endogenous Calpain Inhibitor Calpastatin.” *Neuron* 80 (5): 1175–89.
Yang, Qian, Ronglin Wang, and Lin Zhu. 2019. “Chaperone-Mediated Autophagy.” *Advances in Experimental Medicine and Biology* 1206: 435–52.
Yan, Jingqi, Morgan W. Porch, Brenda Court-Vazquez, Michael V. L. Bennett, and R. Suzanne Zukin. 2018. “Activation of Autophagy Rescues Synaptic and Cognitive Deficits in Fragile X Mice.” *Proceedings of the National Academy of Sciences of the United States of America* 115 (41): E9707–16.
Yu, Xiaomeng M., Itai Gutman, Timothy J. Mosca, Tal Iram, Engin Ozkan, K. Christopher Garcia, Liqun Luo, and Oren Schuldiner. 2013. “Plum, an Immunoglobulin Superfamily Protein, Regulates Axon Pruning by Facilitating TGF-β Signaling.” *Neuron* 78 (3): 456–68.
Zaqout, Sami, and Angela M. Kaindl. 2016. “Golgi-Cox Staining Step by Step.” *Frontiers in Neuroanatomy* 10 (March): 38.

Zecevic, N. 1998. “Synaptogenesis in Layer I of the Human Cerebral Cortex in the First Half of Gestation.” *Cerebral Cortex* 8 (3): 245–52.
Zheng, Xiaoyan, Jian Wang, Theodor E. Haerry, Ann Y-H Wu, Josephine Martin, Michael B. O’Connor, Ching-Hsien J. Lee, and Tzumin Lee. 2003. “TGF-Beta Signaling Activates Steroid Hormone Receptor Expression during Neuronal Remodeling in the Drosophila Brain.” *Cell* 112 (3): 303–15.
Zhou, Qiang, Koichi J. Homma, and Mu-Ming Poo. 2004. “Shrinkage of Dendritic Spines Associated with Long-Term Depression of Hippocampal Synapses.” *Neuron* 44 (5): 749–57.